Maeda, M. and Hino, O. (2006): Molecular tumor markers for asbestos-related mesothelioma: serum diagnostic markers. Pathol. Int., **56**, 649-654.

Ordóñez, N.G. (2003): Value of mesothelin immunostaining in the diagnosis of mesothelioma. Mod. Pathol., **16**, 192-197.

Nakaishi, M., Kajino, K., Ikesue, M., Hagiwara, Y., Kuwahara, M., Mitani, H., Horikoshi-Sakuraba, Y., Segawa, T., Kon, S., Maeda, M., Wang, T., Abe, M., Yokoyama, M. and Hino, O. (2007): Establishment of the enzyme-linked immunosorbent assay system to detect the amino terminal secretary form of rat Erc/Mesothelin. Cancer Sci., **98**, 659-664.

Sakamoto, Y., Nakae, D., Fukumori, N., Tayama, K., Maekawa, A., Imai, K., Hirose, A., Nishimura, T., Ohashi, N. and Ogata, A. (2009): Induction of mesothelioma by a single intrascrotal administration of multi-wall carbon nanotube in intact male Fischer 344 rats. J. Toxicol. Sci., **34**, 65-76.

Shiomi, K., Miyamoto, H., Segawa, T., Hagiwara, Y., Ota, A., Maeda, M., Takahashi, K., Masuda, K., Sakao, Y. and Hino, O. (2006): Novel ELISA system for detection of N-ERC/mesothelin in the sera of mesothelioma patients. Cancer Sci., **97**, 928-932.

Shiomi, K., Hagiwara, Y., Sonoue, K., Segawa, T., Miyashita, K., Maeda, M., Izumi, H., Masuda, K., Hirabayashi, M.,

Moroboshi, T., Yoshiyama, T., Ishida, A., Natori, Y., Inoue, A., Kobayashi, M., Sakao, Y., Miyamoto, H., Takahashi, K. and Hino, O. (2008): Sensitive and specific new enzyme-linked immunosorbent assay for N-ERC/mesothelin increases its potential as a useful serum tumor marker for mesothelioma. Clin. Cancer Res., **14**, 1431-1437.

Tajima, K., Hirama, M., Shiomi, K., Ishiwata, T., Yoshioka, M., Iwase, A., Iwakami, S., Yamazaki, M., Toba, M., Tobino, K., Sugano, K., Ichikawa, M., Hagiwara, Y., Takahashi, K. and Hino, O. (2008): ERC/mesothelin as a marker for chemotherapeutic response in patients with mesothelioma. Anticancer Res., **28**, 3933-3936.

Yamaguchi, N., Hattori, K., Oheda, M., Kojima, T., Imai, N. and Ochi, N. (1994): A novel cytokine exhibiting megakaryocyte potentiating activity from a human pancreatic tumor-cell line HPC-Y5. J. Biol. Chem., **269**, 805-808.

Yamashita, Y., Yokoyama, M., Kobayashi, E., Takai, S. and Hino, O. (2000): Mapping and determination of the cDNA sequence of the *Erc* gene preferentially expressed in renal cell carcinoma in the *Tsc2* gene mutant (Eker) rat model. Biochem. Biophys. Res. Commun., **275**, 134-140.

Involvement of macrophage inflammatory protein 1α (MIP1α) in promotion of rat lung and mammary carcinogenic activity of nanoscale titanium dioxide particles administered by intra-pulmonary spraying

Jiegou Xu[1], Mitsuru Futakuchi[1], Masaaki Iigo[1], Katsumi Fukamachi[1], David B.Alexander[1], Hideo Shimizu[2], Yuto Sakai[1,3], Seiko Tamano[4], Fumio Furukawa[4], Tadashi Uchino[5], Hiroshi Tokunaga[6], Tetsuji Nishimura[5], Akihiko Hirose[5], Jun Kanno[5] and Hiroyuki Tsuda[1,*]

[1]Department of Molecular Toxicology and [2]Core Laboratory, Nagoya City University Graduate School of Medical Sciences, 1-Kawasumi, Mizuho-cho, Mizuho-ku, Nagoya 467-8601, Japan, [3]Department of Drug Metabolism and Disposition, Graduate School of Pharmaceutical Sciences, 3-1, Tanabe-Dohri, Mizuho-ku, Nagoya 467-8603, Japan, [4]DIMS Institute of Medical Science, Inc., 64 Goura, Nishiazai, Azai-cho, Ichinomiya 491-0113, Japan, [5]National Institute of Health Sciences, 1-18-1 Kamiyoga, Setagaya-ku, Tokyo 158-8501, Japan and [6]Pharmaceuticals and Medical Devices Agency, 2-3-3, Kasumigaseki, Chiyoda-ku, Tokyo 100-0013, Japan

*To whom correspondence should be addressed. Tel: +81 52 853 8991; Fax: +81 52 853 8996; Email: htsuda@med.nagoya-cu.ac.jp

Titanium dioxide (TiO$_2$) is evaluated by World Health Organization/International Agency for Research on Cancer as a Group 2B carcinogen. The present study was conducted to detect carcinogenic activity of nanoscale TiO$_2$ administered by a novel intrapulmonary spraying (IPS)-initiation–promotion protocol in the rat lung. Female human c-Ha-*ras* proto-oncogene transgenic rat (H*ras*128) transgenic rats were treated first with *N*-nitrosobis(2-hydroxypropyl)amine (DHPN) in the drinking water and then with TiO$_2$ (rutile type, mean diameter 20 nm, without coating) by IPS. TiO$_2$ treatment significantly increased the multiplicity of DHPN-induced alveolar cell hyperplasias and adenomas in the lung, and the multiplicity of mammary adenocarcinomas, confirming the effectiveness of the IPS-initiation–promotion protocol. TiO$_2$ aggregates were localized exclusively in alveolar macrophages and had a mean diameter of 107.4 nm. To investigate the underlying mechanism of its carcinogenic effects, TiO$_2$ was administered to wild-type rats by IPS five times over 9 days. TiO$_2$ treatment significantly increased 8-hydroxydeoxy guanosine level, superoxide dismutase activity and macrophage inflammatory protein 1α (MIP1α) expression in the lung. MIP1α, detected in the cytoplasm of TiO$_2$-laden alveolar macrophages *in vivo* and in the media of rat primary alveolar macrophages treated with TiO$_2$ *in vitro*, enhanced proliferation of human lung cancer cells. Furthermore, MIP1α, also detected in the sera and mammary adenocarcinomas of TiO$_2$-treated H*ras*128 rats, enhanced proliferation of rat mammary carcinoma cells. These data indicate that secreted MIP1α from TiO$_2$-laden alveolar macrophages can cause cell proliferation in the alveoli and mammary gland and suggest that TiO$_2$ tumor promotion is mediated by MIP1α acting locally in the alveoli and distantly in the mammary gland after transport via the circulation.

Introduction

Inhalation of particles and fiber is well known to be strongly associated with increased lung cancer risk in the workplace (1,2). Although the size of fiber particles was reported to be closely related to risk (3), the precise role of particles and fibers in lung cancer induction has not yet been elucidated.

Titanium dioxide (TiO$_2$) particles of various sizes are manufactured worldwide in large quantities and are used in a wide range of applications. TiO$_2$ particles have long been considered to pose little risk to respiratory health because they are chemically and thermally stable. However, TiO$_2$ is classified as a Group 2B carcinogen, a possible carcinogen to humans, by World Health Organization/International Agency for Research on Cancer based on the findings of lung tumor induction in female rats (3,4). This overall evaluation includes nanoscale (<100 nm in diameter) and larger sized classes of TiO$_2$. At present, the mechanism underlying the development of rat lung tumors by inhalation of TiO$_2$ particles is unclear.

Inhalation of TiO$_2$ particles can occur both at the workplace, e.g. in manufacturing and packing sites, and also outside the workplace during their use (5–7). Exposure to airborne nanoparticles has been reported to be associated with a granulomatous inflammatory response in the lung (8). Inhalation studies of nanoparticles for cancer risk assessment is urgently needed, however, due to the high cost of long-term studies, available data is severely limited (9,10). The aim of this study is to understand the mechanism underlying rat lung carcinogenesis induced by inhalation of TiO$_2$ particles. We choose intrapulmonary spraying (IPS) because it does not require costly facilities, allows accurate dose control and approximates long-term inhalation studies (3,11).

We initially examined whether TiO$_2$ particles have carcinogenic activity in the rat lung using a novel IPS-initiation–promotion protocol (12,13). For these experiments, Sprague–Dawley (SD)-derived female human c-Ha-*ras* proto-oncogene transgenic rat (H*ras*128) transgenic rats, which are known to have the same carcinogen susceptibility phenotype in the lung as wild-type rats but are highly susceptible to mammary tumor induction (14–16), were treated with *N*-nitrosobis(2-hydroxypropyl)amine (DHPN) to initiate carcinogenesis and then treated with TiO$_2$ by IPS. We observed a promotion effect of TiO$_2$ particles in lung and mammary gland carcinogenesis.

To identify factors involved in this promotion effect, wild-type SD strain rats were treated with TiO$_2$ by IPS for 9 days. We found macrophage inflammatory protein 1α (MIP1α) was produced by TiO$_2$-laden alveolar macrophages in the lungs of rats treated with TiO$_2$. MIP1α is a member of the CC chemokine family and is primarily associated with cell adhesion and migration of multiple myeloma cells (17). It is reported to be produced by macrophages in response to a variety of inflammatory stimuli including TiO$_2$ (18). In the present study, MIP1α, detected in the medium of rat primary alveolar macrophages treated with TiO$_2$, enhanced proliferation of human lung cancer cells *in vitro*. MIP1α was also detected in the sera and mammary adenocarcinomas of TiO$_2$-treated H*ras*128 rats and enhanced proliferation of rat mammary carcinoma cells.

Materials and methods

Animals

Female transgenic rats carrying the H*ras*128 and female wild-type SD rats were obtained from CLEA Japan Co., Ltd (Tokyo, Japan) (15). The animals were housed in the animal center of Nagoya City University Medical School, maintained on a 12 h light–dark cycle and received Oriental MF basal diet (Oriental Yeast Co., Tokyo, Japan) and water *ad libitum*. The research was conducted according to the Guidelines for the Care and Use of Laboratory Animals of

Abbreviations: CCR1, C-C chemokine receptor type 1; DHPN, *N*-nitrosobis (2-hydroxypropyl) amine; ERK, extracellular signal-regulated kinase; GRO, growth-regulated oncogene; H*ras*128 rat, human c-Ha-*ras* proto-oncogene transgenic rat; IL, interleukin; IPS, intrapulmonary spraying; MEK1, MAPK/ERK kinase1; MIP1α, macrophage inflammatory protein 1α; 8-OHdG, 8-hydroxydeoxy guanosine; PBS, phosphate-buffered saline; ROS, reactive oxygen species; SD, Sprague–Dawley; SOD, superoxide dismutase; TEM, transmission electron microscopy; TiO$_2$, titanium dioxide.

927

Nagoya City University Medical School and the experimental protocol was approved by the Institutional Animal Care and Use Committee (H17-28).

Preparation of TiO₂ and IPS

TiO₂ particles (rutile type, without coating; with a mean primary size of 20 nm) were provided by Japan Cosmetic Association, Tokyo, Japan. TiO₂ particles were suspended in saline at 250 µg/ml or 500 µg/ml. The suspension was autoclaved and then sonicated for 20 min just before use. The TiO₂ suspension was intratracheally administered to animals under isoflurane anesthesia using a Microsprayer (Series IA-1B Intratracheal Aerosolizer, Penn-Century, Philadelphia, PA) connected to a 1 ml syringe; the nozzle of the sprayer was inserted into the trachea through the larynx and a total of 0.5 ml suspension was sprayed into the lungs synchronizing with spontaneous respiratory inhalation (IPS).

IPS-initiation–promotion protocol

Thirty-three female Hras128 rats aged 6 weeks were given 0.2% DHPN, (Wako Chemicals Co., Ltd Osaka, Japan) in the drinking water for 2 weeks and 9 rats were given drinking water without DHPN. Two weeks later, the rats were divided into four groups, DHPN alone (Group 1), DHPN followed by 250 µg/ml TiO₂ (Group 2), DHPN followed by 500 µg/ml TiO₂ (Group 3) and 500 µg/ml TiO₂ without DHPN (Group 4). The TiO₂ particle preparations were administered by IPS once every 2 weeks from the end of week 4 to week 16 (a total of seven times). The total amount of TiO₂ administered to Groups 1, 2, 3 and 4 were 0, 0.875, 1.75 and 1.75 mg per rat, respectively. Three days after the last treatment, animals were killed and the organs (brain, lung, liver, spleen, kidney, mammary gland, ovaries, uterus and neck lymph nodes) were excised and divided into two pieces; one piece was immediately frozen at −80°C and used for quantitative measurement of elemental titanium, and the other piece was fixed in 4% paraformaldehyde solution in phosphate-buffered saline (PBS) buffer adjusted to pH 7.3 and processed for light microscopic examination and transmission electron microscopy (TEM); the left lungs and inguinal mammary glands were used for elemental titanium analysis and the right lungs and inguinal mammary glands were used for microscopic examination.

IPS 9 day protocol

Twenty female SD rats (wild-type counterpart of Hras128) aged 10 weeks were treated by IPS with 0.5 ml suspension of 500 µg/ml TiO₂ particles in saline five times over a 9 day period (Figure 2A). The total amount of TiO₂ administered was 1.25 mg per rat. Six hours after the last dose, animals were killed and the lungs and inguinal mammary glands were excised. Fatty tissue surrounding the mammary gland was removed as much as possible. The left lungs and inguinal mammary glands were used for biochemical analysis, and the right lungs were fixed in 4% paraformaldehyde solution in PBS adjusted at pH 7.3 and processed for histopathological examination and immunohistochemistry.

Light microscopic and TEM observation of TiO₂ particles in the lung

Paraffin blocks were deparaffinized and embedded in epon resin and processed for TiO₂ particle observation and titanium element analysis, using a JEM-1010 transmission electron microscope (JEOL Co. Ltd, Tokyo, Japan) equipped with an X-ray microanalyzer (EDAX, Tokyo, Japan). Size analysis of TiO₂ particles was performed using TEM photos by an image analyzer system, (IPAP, Sumika Technos Corporation, Osaka, Japan). A total of 452 particles from alveolar macrophages from rats in Group 3 (DHPN followed by 500 µg/ml TiO₂) of the IPS-initiation–promotion study and a total of 2571 particles from alveolar macrophages from rats in the IPS 9 day study were measured.

Biochemical element analysis of titanium

For the detection of elemental titanium, frozen tissue samples of 50–100 mg were digested with 5 ml concentrated HNO_3 for 22 min in a microwave oven. Titanium in the digested solutions was determined by inductively coupled plasma–mass spectrometry (HP-4500, Hewlett-Packard Co., Houston, TX) under the following conditions: RF power, 1450 W; RF refraction current, 5 W; Plasma gas current, 15 l/min; Carrier gas current, 0.91 l/min; Peri pump, 0.2 r.p.s.; Monitoring mass-m/z 48 (Ti); Integrating interval, 0.1 s; Sampling period 0.31 s.

Analysis of superoxide dismutase activity, 8-hydroxydeoxy guanosine and cytokine levels

For the analysis of superoxide dismutase (SOD) activity, 8-hydroxydeoxy guanosine (8-OHdG) and cytokine levels, animals exposed to TiO₂ particles for 9 days were used. For 8-OHdG levels, genomic DNA was isolated from the left lung and inguinal mammary gland with a DNA Extractor WB Kit (Wako Chemicals Co. Ltd). 8-OHdG levels were determined with an 8-OHdG ELISA Check Kit (Japan Institute for the Control of Aging, Shizuoka, Japan) and by a custom service (OHG Institute Co., Ltd, Fukuoka, Japan). For the analysis of SOD activity and inflammation-related cytokines, tissue from the left lung and inguinal mammary glands was excised and rinsed with cold PBS three times

and homogenized in 1 ml of T-PER, Tissue Protein Extraction Reagent (Pierce, Rockford, IL), containing 1% (vol/vol) proteinase inhibitor cocktail (Sigma–Aldrich, St Louis, MO). The homogenates were clarified by centrifugation at 10 000g for 5 min at 4°C. Protein content was measured using a BCA™ Protein Assay Kit (Pierce). SOD activity was determined using an SOD Assay Kit (Cayman Chemical Co., Ann Arbor, MI). The levels of interleukin (IL)-1α, IL-1β, IL-6, granulocyte-macrophage colony-stimulating factor, granulocyte colony-stimulating factor, tumor necrosis factor α, interferon γ, IL-18, monocyte chemotactic protein 1 and MIP1α, growth-regulated oncogene (GRO) and vascular endothelial growth factor were measured by Multiplex Suspension array (GeneticLab Co., Ltd, Sapporo, Japan).

Immunohistochemistry

CD68 and MIP1α were detected using anti-rat CD68 (BMA Biomedicals, Augst, Switzerland) and anti-rat MIP1α polyclonal antibodies (BioVision, Lyon, France). Both antibodies were diluted 1:100 in blocking solution and applied to slides, and the slides were incubated at 4°C overnight. The slides were then incubated for 1 h with biotinylated species-specific secondary antibodies diluted 1:500 (Vector Laboratories, Burlingame, CA) and visualized using avidin-conjugated alkaline phosphatase complex (ABC kit, Vector Laboratories) and Alkaline Phosphatase Substrate Kit (Vector Laboratories).

Isolation of primary alveolar macrophages and preparation of conditioned media

Wild-type female SD rats were given 0.5 ml 6% thioglycollate medium (Thioglycollate Medium II, Eiken Chemical Co., Ltd, Tokyo, Japan) by IPS on days 1, 3 and 5, and 6 h after the last treatment, the lungs were excised and minced with sterilized scissors in RPMI 1640 containing 10% fetal bovine serum (Wako Chemicals Co., Ltd) and antibiotics. The homogenate was washed twice and plated onto 6 cm dishes and incubated for 2 h at 37°C, 5% CO₂. The dishes were then washed with PBS three times to remove unattached cells and cell debris. Samples of the remaining adherent cells were cultured in chamber slides and immunostained for CD68 to confirm their identity as macrophages; ~98% of the cells were positive for CD68.

Primary alveolar macrophages were treated with vehicle or TiO₂ particles in saline suspension at a final concentration of 100 µg/ml and then incubated for 24 h in a 37°C, 5% CO₂ incubator. The conditioned medium was collected and diluted 5-fold with RPMI 1640; the conditioned medium had a final concentration of 2% fetal bovine serum.

Western blotting

For the detection of MIP1α, aliquots of 20 µg protein from the extracts of lung or mammary tissue were separated by 15% sodium dodecyl sulfate–polyacrylamide gel electrophoresis, transferred to nitrocellulose membranes and immunoblotted. For the detection of C-C chemokine receptor type 1 (CCR1), 10% sodium dodecyl sulfate–polyacrylamide gel electrophoresis was used for the separation. Membranes were probed overnight at 4°C with anti-rat MIP1α polyclonal antibody (BioVision) diluted at 1:100 or anti-CCR1 (Santa Cruz Biotechnology, Santa Cruz, CA) diluted at 1:100. The blots were washed and incubated for 1 h with biotinylated anti-species-specific secondary antibodies (Amersham Biosciences, Piscataway, NJ) and then visualized using ECL Western Blotting Detection Reagent (Amersham Biosciences). To ensure equal protein loading, the blots were striped with Restore Western Blot Stripping Buffer (Pierce) and reprobed with anti-β actin antibody (dilution 1:2000; Sigma–Aldrich) for 1 h at room temperature.

For the detection of serum MIP1α, GRO and IL-6, aliquots of 150 µg of protein from the sera of rats treated with TiO₂ for 16 weeks were subjected to sodium dodecyl sulfate–polyacrylamide gel electrophoresis. Anti-human GRO polyclonal antibody (BioVision) and anti-mouse IL-6 polyclonal antibody (Santa Cruz) were diluted 1:100. For detection of activated extracellular signal-regulated kinase (ERK) 1/2 and total ERK1/2, phospho ERK1/2 antiboby (Cell signaling Technology, Beverly, MA) and ERK1/2 antibody (Upstate, Lake placid, NY) were diluted 1:2000 and 1:25 000, respectively. The conditioned medium from alveolar macrophages, prepared as described above, was also subjected to western blot assay for MIP1α detection as described above. The blots were striped with Restore Western Blot Stripping Buffer (Pierce) and stained with Ponceau S solution (Sigma–Aldrich) for 10 min. The major band at 66 kDa was judged to be albumin and used as an internal control.

In vitro cell proliferation assay

A549 cells, a human lung cancer cell line, and the rat mammary cancer cell line C3 (19), derived from the Hras128 transgenic rats, were used in the *in vitro* cell proliferation assays. A549 or C3 cells were seeded into 96-well culture plates at 5 × 10³ cells per well in 2% fetal bovine serum Dulbecco's modified Eagle's medium (Wako Chemicals Co., Ltd). After overnight incubation, the cells were treated as noted below, incubated for 72 h and the relative cell number was then determined.

928

To investigate the effect of culture supernatant from alveolar macrophages on A549 cell proliferation, their media were replaced with diluted conditioned medium, and the cells were incubated for 72 h with 0, 5, 10 and 20 µg/ml of anti-MIP1α neutralizing antibody (R&D Systems, Minneapolis, MN) or with 20 µg/ml of irrelevant IgG. To investigate the effect of recombinant cytokines on A549 cell proliferation, 10, 50 or 100 ng/ml of recombinant protein, rat MIP1α (R&D Systems), human GRO (R&D Systems) or human IL-6 (R&D Systems), was added to A549 cells. To investigate the role of ERK in MIP1α-stimulated cell proliferation, A549 cells, treated with or without 2×10^{-7} M of the specific MAPK/ERK kinase1 (MEK1) inhibitor PD98059 (Cell Signaling Technology) for 10 min, were treated with 50 ng/ml of MIP1α protein. To investigate the effect of reactive oxygen species (ROS) on cell proliferation, A549 cells, with or without pretreatment with 1 mM N-acetyl cysteine (Wako Chemicals Co. Ltd) for 30 min, were treated with 0.5 mM H_2O_2 (Wako Chemicals Co. Ltd). To investigate of the effects of MIP1α on rat mammary cells, C3 cells were treated with serially diluted recombinant rat MIP1α (0, 0.4, 2.0, 10 and 50 ng/ml, respectively; R&D Systems). For detecting the direct effect of TiO₂ particles on A549 and C3 cell proliferation, 5×10^3 A549 or C3 cells were cultured overnight and then treated with 10 or 50 µg/ml of TiO₂ particles.

After 72 h incubation, the relative cell number of A549 and C3 was determined using the Cell Counting Kit-8 (Dojindo Molecular Technologies, Rockville, MD) according to the manufacturer's instruction.

Statistical analysis

For *in vivo* data, statistical analysis was performed using the Kruskal–Wallis and Bonferroni–Dunn's multiple comparison tests. *In vitro* data are presented as means ± standard deviations. The statistical significance of *in vitro* findings was analyzed using a two-tailed Student's *t*-test and Bonferroni–Dunn's multiple comparison tests. A value of $P < 0.05$ was considered significant. The Spearman's rank correlation test was used to determine the association between TiO₂ dose and TiO₂ carcinogenic activity.

Results

Promoting effects of TiO₂ particles in DHPN-induced lung and mammary carcinogenesis

Prior to initiation of the IPS-initiation–promotion and IPS 9 day studies, we conducted a preliminary study to confirm whether IPS would be a good tool to deliver TiO₂ particles to the alveoli. Rats were treated by IPS with India ink. We observed that ink particles of ~50 to 500 µm in diameter were diffusely distributed throughout the alveoli space (data not shown), confirming that IPS could deliver TiO₂ particles to the alveoli.

Four groups of female Hras128 rats were treated with +/− DHPN to initiate carcinogenesis and then treated with TiO₂ by IPS for 12 weeks: Group 1, DHPN alone; Group 2, DHPN followed by 250 µg/ml TiO₂; Group 3, DHPN followed by 500 µg/ml TiO₂ and Group 4, 500 µg/ml TiO₂ without DHPN. Microscopic observation in the lung showed scattered inflammatory foci, alveolar cell hyperplasia (Figure 1A) and adenomas in the DHPN-treated rats. The multiplicity (numbers per square centimeter lung) of hyperplasias and adenomas in Group 3 (DHPN followed by 500 µg/ml TiO₂) were significantly increased compared with Group 1 (DHPN followed by saline, Table I), and the increase showed a dose-dependent correlation (rho = 0.630, $P = 0.001$ for hyperplasias and rho = 0.592, $P = 0.029$ for adenomas) by the Spearman's rank correlation test. In the mammary gland, TiO₂ treatment significantly increased the multiplicity of adenocarcinomas (Figure 1C) and tended to increase the weight of the mammary tumors (Figure 1C). In the rats, which received TiO₂ treatment without prior DHPN treatment, alveolar proliferative lesions were not observed although slight inflammatory lesions were observed.

TiO₂ was distributed primarily to the lung, but minor amounts of TiO₂ were also found in other organs (supplementary Figure 1A is available at *Carcinogenesis* Online).

Various sizes of TiO₂ aggregates were observed in alveolar macrophages (Figure 1B). The TiO₂-laden macrophages were evenly scattered throughout the lung alveoli. The number of hyperplasias with TiO₂-laden macrophages was dose dependently increased (supplementary Table 1 is available at *Carcinogenesis* Online). This result suggests that TiO₂-laden macrophages may be involved in the promotion of alveolar hyperplasia.

The size distribution of TiO₂ particle aggregate is shown in Figure 1D. Of 452 particle aggregates examined, 362 (80.1%) were nanosize, i.e.

<100 nm. Overall, the average size was 84.9 nm and the median size was 44.4 nm.

IPS 9 day study—analysis of TiO₂

Female SD rats were treated with TiO₂ by IPS over a 9 day period (Figure 2A). Microscopic observation showed scattered inflammatory lesions with infiltration of numerous macrophages mixed with a few neutrophils and lymphocytes in TiO₂-treated animals. Overall, the number of macrophages in the alveoli was significantly increased in the TiO₂-treated animals (Figure 2B). As expected from the results of the IPS-initiation–promotion study, alveolar proliferative lesions were not observed (Figure 2C).

Morphologically, TiO₂ particles were observed as yellowish, polygonal bodies in the cytoplasm of cells (Figure 2D). These cells are morphologically distinct from neutrophils and strongly positive for CD68 (Figure 2E), indicating that the TiO₂ engulfing cells were macrophages. TiO₂ aggregates of various sizes were found in macrophages, and aggregates larger than a single macrophage were surrounded by multiple macrophages (supplementary Figure 1B is available at *Carcinogenesis* Online)

TEM also showed electron dense bodies in the cytoplasm of macrophages (Figure 2F and G). These bodies were found exclusively in macrophages and not found in the alveolar parenchyma, including alveolar epithelium and alveolar wall cells, or in any other cell type. The shape of the electron dense TiO₂ particles in the cytoplasm was quite similar to that observed in preparations taken from TiO₂ suspensions before administration (Figure 2H and supplementary Figure 1C and D is available at *Carcinogenesis* Online). Individual TiO₂ particles were rod-like in shape (supplementary Figure 1C is available at *Carcinogenesis* Online).

Element analysis by TEM and X-ray microanalysis indicated that these electron dense bodies were composed primarily of titanium particles (supplementary Figure 1E and F-1 and 1F-2 is available at *Carcinogenesis* Online). Titanium was not observed in the surrounding alveolar cells without electron dense bodies (supplementary Figure 1F-3 is available at *Carcinogenesis* Online). The size distribution of TiO₂ particle aggregates is shown in Figure 2I. Of 2571 particle aggregates examined, 1970 (76.6%) were <100 nm and five particles were >4000 nm in size. Overall, the average size was 107.4 nm and the median size was 48.1 nm.

IPS 9 day study—analysis of oxidative stress and inflammation-related factors in the lungs of wild-type rats

IPS of TiO₂ particles significantly increased SOD activity (Figure 3A) and 8-OHdG levels (Figure 3B) in the lungs of wild-type rats, but not in the mammary glands. Analysis of the expression levels of 12 cytokines using suspension array indicated that administration of TiO₂ particles significantly upregulated the expression of MIP1α, GRO and IL-6 in the lung tissue of wild-type rats (supplementary Table 2 is available at *Carcinogenesis* Online). MIP1α levels were slightly elevated (0.4 pg/mg protein) in the mammary gland (Figure 3C), although the elevation was not statistically significant. Elevation of MIP1α in the lung tissue of animals treated with TiO₂ particles was confirmed by western blotting (Figure 3D).

Immunohistochemically, MIP1α was detected in the cytoplasm of alveolar macrophages with phagocytosed TiO₂ particles (Figure 3E upper, stained in red) and these macrophages could be found in hyperplastic lesions of the lung (supplementary Figure 2A and B is available at *Carcinogenesis* Online). MIP1α was not detected in macrophages without TiO₂ particles (Figure 3E lower). Expression of CCR1, the major receptor of MIP1α, was observed in the lung; IPS of TiO₂ particles had little or no effect on CCR1 expression (supplementary Figure 2C is available at *Carcinogenesis* Online).

Effect of MIP1α on proliferation of a human lung cancer cell line in vitro

Alveolar macrophages were isolated from the lungs of SD rats and were confirmed to be macrophages by morphology and CD68 staining
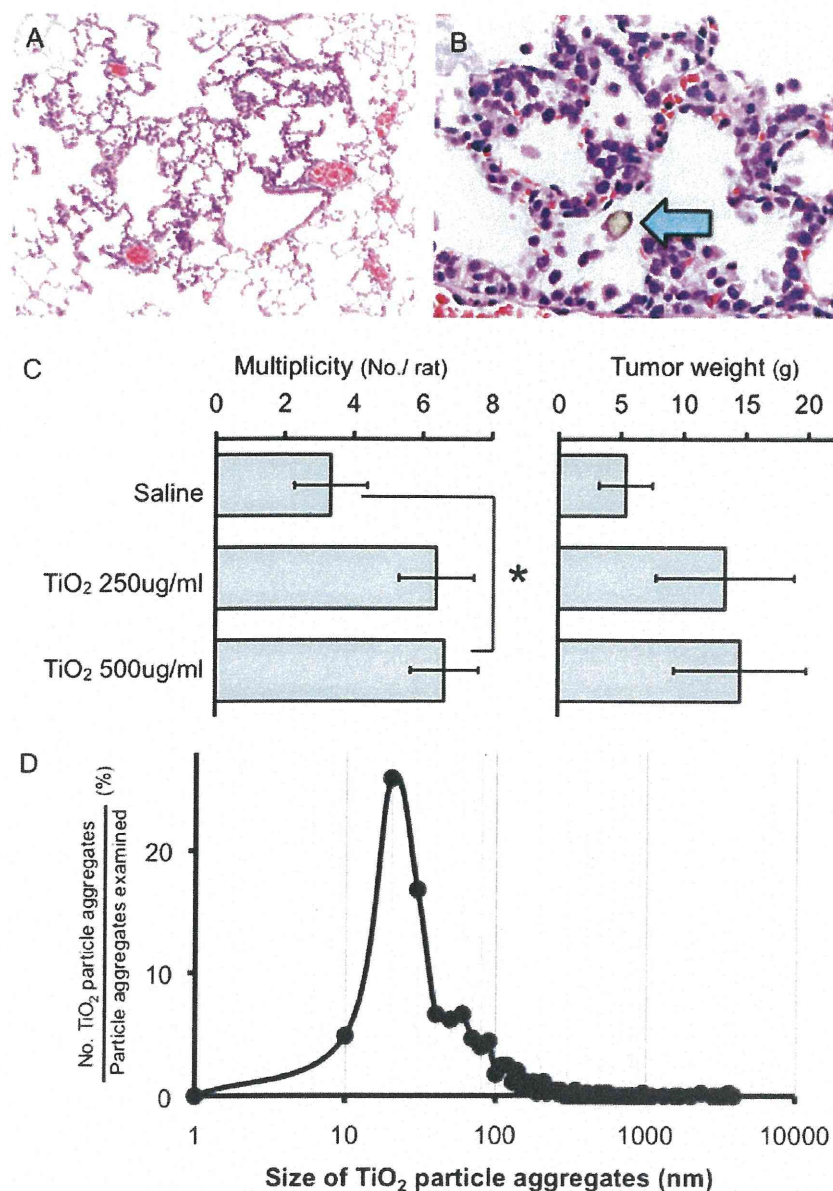
929

Fig. 1. Promoting effects of TiO$_2$ particles in DHPN-induced lung and mammary carcinogenesis (**A**) Alveolar hyperplasias observed in the lung of an Hras128 rat receiving DHPN and 500 μg/ml TiO$_2$ particles. (**B**) Alveolar macrophages with TiO$_2$ particles were also observed in hyperplasia lesions. (**C**) IPS of TiO$_2$ particles significantly increased the multiplicity of adenocarcinomas in the mammary gland and tended to increase the size of mammary tumors. (**D**) The size distribution of TiO$_2$ particle aggregates; among 452 particle aggregates examined, 362 (80.1%) were nanosize, i.e. <100 nm in diameter.

(data not shown). The macrophages were treated with TiO$_2$ particles suspended in saline (Figure 4A). TiO$_2$ induced secretion of MIP1α into the culture media (Figure 4B), and the culture medium collected from macrophages treated with TiO$_2$ particles promoted proliferation of A549 cells, whereas culture media collected from unexposed macrophages did not (Figure 4C). MIP1α neutralizing antibodies attenuated the promotion of A549 proliferation in a dose-dependent manner (Figure 4C). MIP1α-induced cell proliferation was also significantly suppressed by the ERK inhibitor PD98059 (Figure 4D). In addition, MIP1α increased ERK phosphorylation and PD98059 diminished ERK phosphorylation (Figure 4E).

We also examined the effect of MIP1α, GRO and IL-6, H$_2$O$_2$ and TiO$_2$ on the proliferation of A549 cells. MIP1α increased cell proliferation in a dose-dependent fashion, but GRO and IL-6 did not

(supplementary Figure 3A–C is available at *Carcinogenesis* Online). H$_2$O$_2$ significantly suppressed cell proliferation, and antioxidant treatment diminished this suppression. Antioxidant treatment did not affect MIP1α-induced cell proliferation (supplementary Figure 3D is available at *Carcinogenesis* Online). These results suggest that ROS have no effect on tumor cell growth in this experiment.

In addition, TiO$_2$ did not directly increase proliferation of A549 cell (supplementary Figure 3E is available at *Carcinogenesis* Online).

Mechanism analysis of the promotion of mammary carcinogenesis

MIP1α was markedly elevated in the serum of the Hras128 rats treated with TiO$_2$ particles (Figure 5A). Serum levels of IL-6 were not changed by TiO$_2$ treatment and GRO was not detected in the serum

930

Table I. Effect of TiO2 on incidence and multiplicity of DHPN-induced alveolar hyperplasia and adenoma of the lung

Treatment	No. of rats	Alveolar hyperplasia		Lung adenoma	
		Incidence (%)	Multiplicity ## (no./cm²)	Incidence (%)	Multiplicity # (no./cm²)
Saline	9	9 (100)	5.91 ± 1.19	0	0
nTiO₂ 250 mg/ml	10	10 (100)	$7.36 \pm 0.97^*$	1 (10)	0.10 ± 0.10
nTiO₂ 500 mg/ml	11	11 (100)	$11.05 \pm 0.87^{**}$	4 (36)	$0.46 \pm 0.21^*$

$^*P < 0.05$, $^{**}P < 0.001$ versus saline control.
$\#P < 0.05$, $\#\#P < 0.001$ in trend test (Spearman's rank correlation test).

(Figure 5A). MIP1α was slightly elevated in the mammary glands of these animals (Figure 5B); possibly, the elevated MIP1α detected in the mammary tissue was due to contamination by MIP1α in the serum. Recombinant MIP1α promoted the proliferation of C3 cells in a dose-dependent manner; a slight induction could be seen at a dose of 400 pg/ml and became statistically significant at the dose of 50 ng/ml (Figure 5C). Expression of CCR1, the major receptor of MIP1α, was observed in mammary tissue, and as in the lung, IPS of TiO₂ particles had little or no effect on CCR1 expression (data not shown). TiO₂ did not directly increase proliferation of C3 cells (supplementary Figure 3F is available at *Carcinogenesis* Online).

Discussion

To elucidate the mechanism underlying rat lung carcinogenesis by TiO₂ inhalation, we chose IPS. Although this method may be less physiological than the aerosol inhalation system, we observed that agglomerates and aggregates of TiO₂ particles from nano to micro size (mean diameter 107.4 nm) were diffusely distributed throughout the lung including peripheral alveoli, and they did not cause obstruction of the terminal bronchioles. Accordingly, IPS of TiO₂ particles can be expected to act similarly to aerosol inhalation of TiO₂.

Occupational exposure limits for TiO₂ in 13 countries or regions are 5–20 mg/m³ (20), which results in TiO₂ exposure limits of 0.27–1.07 mg/kg body wt/day; calculations based on the human respiratory volume. In the present study, a total of 1.75 mg was administered per rat for 12 weeks in the high-dose group, resulting in a dose of 0.104 mg/kg body wt/day. Therefore, the dose we used in the present study was lower than the occupational exposure limit.

TiO₂, nanoscale and larger sized is evaluated as a Group 2B carcinogen by World Health Organization/International Agency for Research on Cancer (4) based on 2 year animal aerosol inhalation studies (3). We conducted the present carcinogenesis study using a two-step initiation–promotion protocol as a surrogate for a 2 year long-term protocol. Our study demonstrated that TiO₂ particles increased the multiplicity of alveolar cell hyperplasia and adenoma in the two-step IPS-initiation–promotion protocol. We used these lesions as endpoints in carcinogenicity testing because chemically induced tumors appear to be derived from hyperplasic lesions that progress to adenoma and carcinoma (21).

Several bioassay protocols based on the two-step carcinogenesis theory have been developed as practical and sensitive assays, and the compounds that exhibit promotion activity are considered to be carcinogens (22–29). Thus, our experimental design may be a practical surrogate for the long-term lung carcinogenesis protocol.

It should be noted that proliferative lesions including alveolar cell hyperplasia and adenomas were not found in the groups subjected to TiO₂ particle administration without prior treatment of DHPN. This is due to the weak carcinogenic potential and short duration of exposure to TiO₂ particles. Using the two-step IPS-initiation–promotion protocol, however, we did observe carcinogenic activity by this weak carcinogen. Thus, the two-step IPS-initiation–promotion protocol is an appropriate system to study carcinogenesis of TiO₂ particles and approximates long-term TiO₂ inhalation studies (3,11).

We next conducted a mechanism analysis of TiO₂ particle carcinogenesis focusing on the initial events induced by exposure to TiO₂ particles. Treatment with TiO₂ resulted in a modest infiltration of inflammatory cells into the alveolar space and septal wall, but the primary effect was a marked increase in the number of macrophages in the alveoli, and many of these macrophages contained phagocytosed TiO₂ particles. Alveolar macrophages play an important role in deposition and clearance of mineral fibers/particles, and macrophage activity is known to be strongly associated with inflammatory reactions and carcinogenesis caused by fibers and particles in the lung, including asbestos (30–33). ROS are known to be produced by macrophages upon particle phagocytosis (34,35). Clinical and experimental studies indicate that ROS production and resultant oxidative stress play an important role in cellular and tissue damage, inflammation and fibrosis in the lung. In our study, a significant increase in the activity of SOD and 8-OHdG formation in the lung were observed, indicating increased ROS production and DNA damage. Because macrophages are unable to detoxify TiO₂ particles, the reaction against these particles would be continuous over an extended period of time. This condition is associated with high levels of ROS production (36) and tissue toxicity (37).

Cytokine analysis of the lung tissue indicated that among the 12 cytokines examined, expression of IL-6, GRO and MIP1α were significantly higher in the TiO₂-treated group than in the vehicle group (supplementary Table 1 is available at *Carcinogenesis* Online). IL-6 is a pro-inflammatory cytokine that is involved in host defense as well as cancer development (38,39). IL-6 has been shown to be increased in lung tumor tissue (40,41) and in the sera of lung cancer patients (42). GRO, a member of the CXC chemokine family, has been shown to be involved in inflammatory responses, chemoattraction (43), carcinogenesis (44,45) and tumor progression (46). Thus, IL-6 and GRO may be involved in the promotion of lung carcinogenesis by TiO₂ (47).

Of the three cytokines induced by exposure to TiO₂ particles, however, we were particularly interested in MIP1α. This cytokine was not only induced in the lung tissue of TiO₂-treated rats, but, unlike IL-6 and GRO, it was also found in the serum of these animals. MIP1α is a member of the CC chemokine family and is primarily associated with cell adhesion and migration (17), proliferation and survival of myeloma cells (48). It is produced by macrophages in response to a variety of mineral particle-induced inflammatory stimuli (18). Our results indicate that expression of MIP1α by alveolar macrophages enhances the proliferation of A549 cells. Expression of CCR1, the major receptor of MIP1α, was observed in the lung tissue, rendering lung cells receptive to MIP1α induction of proliferation. Lung damage and inflammation induced by TiO₂ particles has also been reported to be associated with increased cell proliferation of lung epithelium cells (49), which is consistent with our results.

The MEK1–ERK-signaling pathway has been shown to be involved in CCR1 signaling (48). In the present study, the MEK1-specific inhibitor PD98059 suppressed MIP1α-induced cell proliferation and ERK phosphorylation. These results suggest that MEK1 is one of the downstream signaling molecules of MIP1α and the MEK1–ERK-signaling pathway may be partially involved in MIP1α signaling.

It should be noted that, in our IPS-initiation–promotion protocol, TiO₂ exposure also promoted DHPN-initiated mammary carcinogenesis. Our results suggest that MIP1α secreted by alveolar macrophages and transported via the circulatory system caused
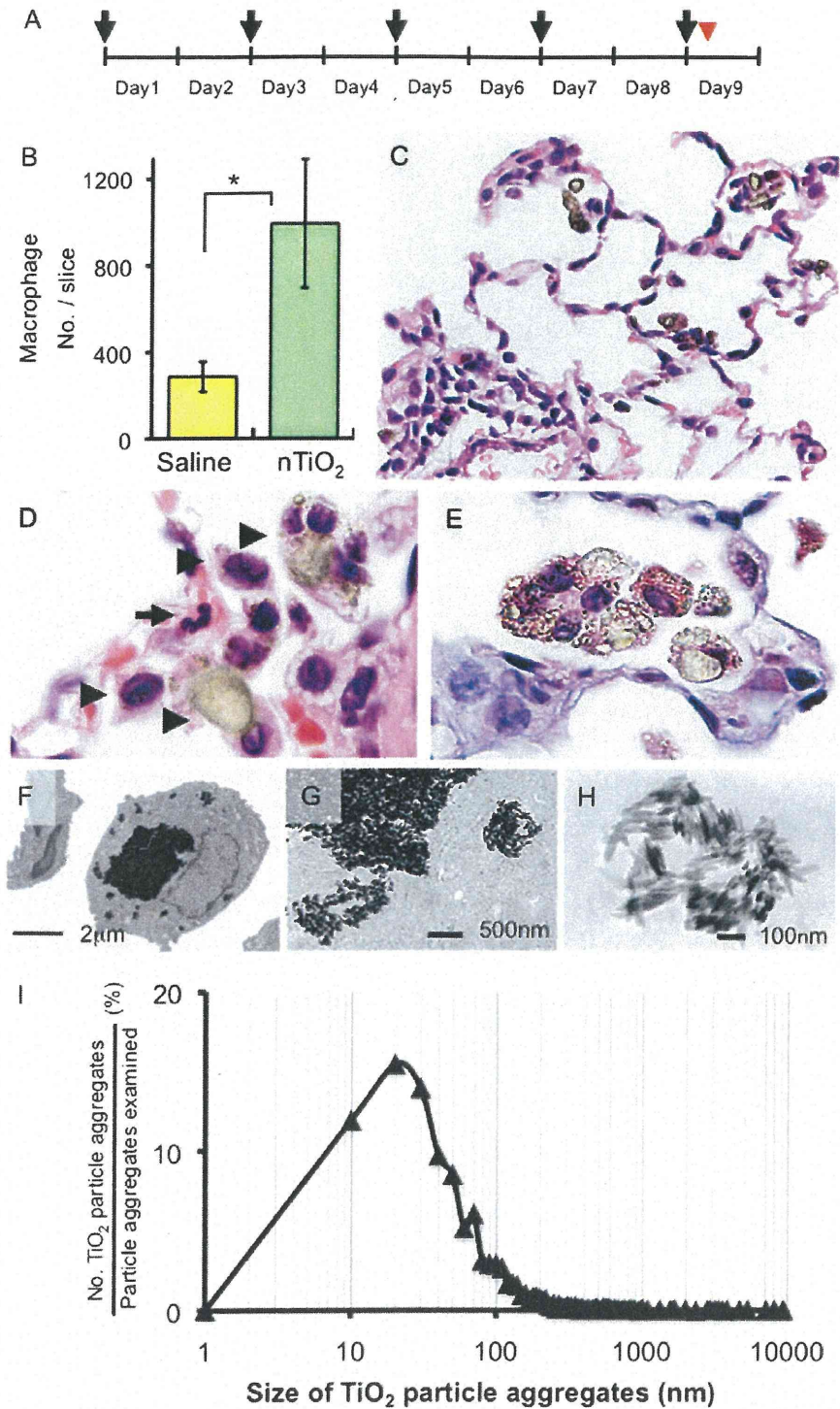
931

Fig. 2. TiO$_2$ particles in alveolar macrophages by light and electron microscopy (A) Twenty female SD rats (wild-type counterpart of H*ras*128) aged 10 weeks were treated by IPS with 0.5 ml suspension of 500 µg/ml TiO$_2$ particles in saline five times over a 9 day period. Arrows and arrowhead indicates IPS treatment and killing of the animals, respectively. (**B**) IPS of TiO$_2$ particles significantly increased the number of macrophages in the alveoli. (**C**) Inflammatory reactions were observed in the lung with slight infiltration of macrophages, neutrophils and lymphocytes. (**D**) TiO$_2$ particles were observed in alveolar macrophages (hematoxylin and eosin staining). Arrowheads indicate macrophages and the smaller cell indicated by the arrow is a neutrophil with its characteristic multilobular nucleus. (**E**) The multinucleated cells containing these particles were positive for the macrophage marker CD68 (Alkaline phosphatase reaction, red color). (**F**) TEM findings showed that TiO$_2$ particles of various sizes (~50 nm to 5 µm) were observed phagocytosed by alveolar macrophages. (**G**) Electron dense bodies were aggregates of TiO$_2$ particles. (**H**) TEM findings of TiO$_2$ particles in saline suspension before IPS. The shape of the TiO$_2$ particle aggregates was similar to those observed in macrophages. (**I**) The size distribution of TiO$_2$ particle aggregates: of 2571 particle aggregates examined, 1970 (77.1%) were <100 nm. The average size was 107.4 nm and the median size was 48.1 nm.
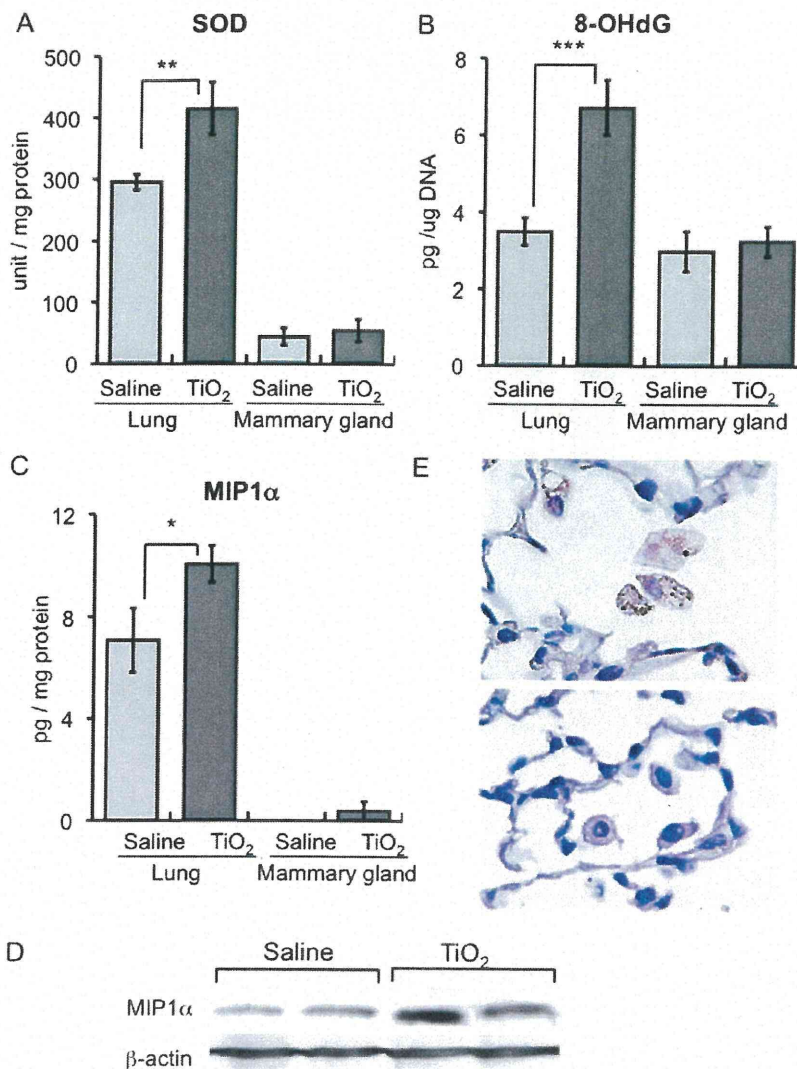
932

Fig. 3. Inflammatory factors upregulated in the lungs of wild-type rats by IT-spraying of TiO₂ particles in the IPS 9 day study (A) SOD activity and (B) 8-OHdG level in wild-type rats treated with TiO₂ particles or saline. (C) MIP1α protein level was significantly increased (142%) in the lung tissue of wild-type rats treated with TiO₂ (suspension array analysis). MIP1α was detected in the mammary gland of the TiO₂ group but not in the vehicle group. (D) In western blotting, expression of MIP1α was increased in the TiO₂ group compared with vehicle group. (E) MIP1α was immunohistochemically detected in alveolar macrophages containing TiO₂ particles (upper) but was not detected in macrophages of rats that were not exposed to TiO₂ particles (lower).

proliferation of mammary epithelial cells and thereby promoted mammary carcinogenesis. As with the lung, CCR1 was expressed by mammary cells, rendering these cells receptive to MIP1α induction of proliferation. While MIP1α secreted by alveolar macrophages would be diluted by the blood volume and while these levels may not be high enough to increase mammary cell proliferation in a short *in vitro* proliferation assay, it is possible that continuous low level stimulation over the course of 12 weeks could increase mammary cell proliferation in the environment of the mammary gland *in vivo*. Another possibility is that TiO₂ particles may act directly on the mammary gland after translocation to the mammary gland from the lung. However, TiO₂ exposure of mammary carcinoma cells did not induce proliferation *in vitro*. It must be understood that promotion of DHPN-induced mammary carcinogenesis by TiO₂ particles was observed in Hras128 female rats, and these animals are very highly susceptible to mammary carcinogenesis (50). Although, the effects we observed on promotion of mammary carcinogenesis in these animals may not be directly relevant to most humans, people at high risk for mammary

carcinogenesis, such as individuals harboring BRCA mutations, may be a relevant population as regards the risk presented by nanoscale TiO₂.

Although our observations are based on results obtained with a mixed population of nanoscale and larger sized particle aggregates, size analysis indicated that 80.1% of them were nanoscale (<100 nm in diameter) in the 16 week IPS-initiation–promotion study and 76.6% were nanoscale in the IPS 9 day study. Thus, the results can be interpreted as being strongly associated with nanoscale particle aggregates.

In conclusion, the IPS-initiation–promotion protocol detected TiO₂ carcinogenic activity in the rat lung and is therefore comparable, at least for TiO₂ inhalation, to a long-term whole body inhalation carcinogenesis study. We also elucidated a plausible mechanism for the carcinogenic effect of TiO₂ particles in the rat lung. Phagocytosis of TiO₂ particles by alveolar macrophages resulted in ROS production and DNA damage and increased expression of MIP1α. MIP1α in turn was able to enhance proliferation of lung epithelium cells. Thus, lung
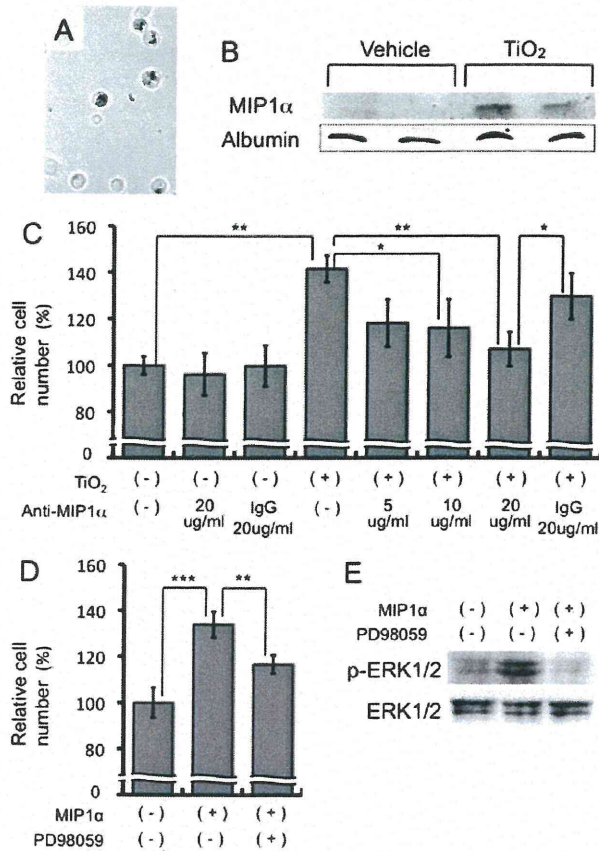
933

Fig. 4. Growth stimulation effects of conditioned medium from alveolar macrophages on human lung cancer cell lines. (**A**) Primary cultured alveolar macrophages of rats were treated with TiO₂ particles. (**B**) MIP1α was detected in the culture medium. (**C**) The number of A549 cells was significantly increased by addition of conditioned medium from alveolar macrophages treated with TiO₂ particles. MIP1α neutralizing antibody attenuated this effect in a dose-dependent manner. Irrelevant IgG was used as control antibody. (**D**) MIP1α-induced cell proliferation was significantly suppressed by the ERK inhibitor PD98059. (**E**) MIP1α increased ERK phosphorylation and PD98059 diminished this phosphorylation.
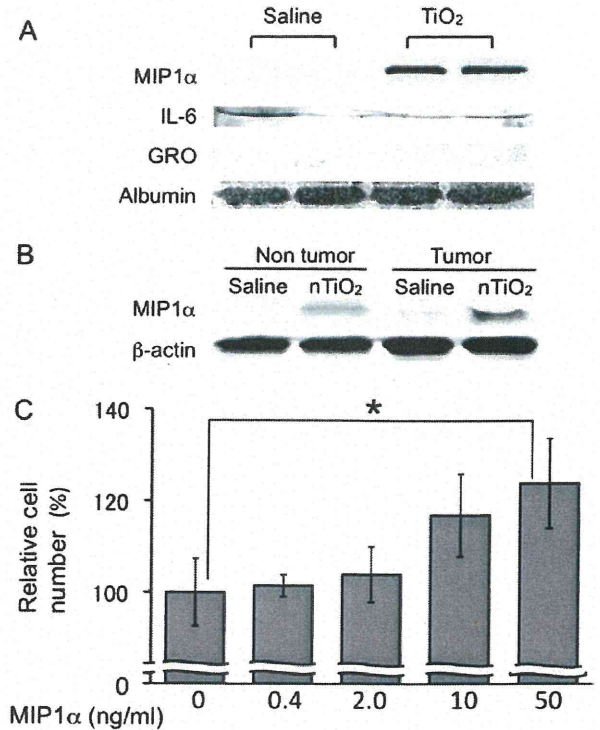
Fig. 5. Promotion effects of MIP1α on proliferation of a rat mammary cancer cell line, C3 (**A**) MIP1α was detected in the serum of the Hras128 rats treated with TiO₂ but not in vehicle control rats in the 16 week study. No difference in IL-6 in the serum was observed and GRO was not detected in the serum. (**B**) MIP1α levels are slightly elevated in non-tumor and tumor tissue of the mammary gland of animals treated by IPS with TiO₂ particles in the 16 week study. (**C**) Recombinant MIP1α increased the number of rat mammary carcinoma C3 cells in a dose-dependent manner ($P = 0.0127$).

tissue exposed to TiO₂ particles exhibits increase in both DNA damage and proliferation. Importantly, a similar mechanism would function in humans in the promotion of lung carcinogenesis associated with inhalation of TiO₂ particles and other nanoparticles with the capacity to form aggregates. In addition, TiO₂ administered to the lung had carcinogenic activity in the Hras128 transgenic rat mammary gland; this carcinogenic activity is probably mediated via serum MIP1α resulting from expression of MIP1α by alveolar macrophages. This finding may indicate that exposure of TiO₂ particles is a risk factor for mammary carcinogenesis in predisposed populations, such as individuals with BRCA mutations.

Supplementary material

Supplementary Figures 1–3 and Tables 1 and 2 can be found at http://carcin.oxfordjournals.org/

References

1. Oberdorster,G. (2002) Toxicokinetics and effects of fibrous and nonfibrous particles. *Inhal. Toxicol.*, **14**, 29–56.
2. Romundstad,P. *et al.* (2001) Cancer incidence among workers in the Norwegian silicon carbide industry. *Am. J. Epidemiol.*, **153**, 978–986.
3. Pott,F. *et al.* (2005) Carcinogenicity study with nineteen granular dusts in rats. *Eur. J. Oncol.*, **10**, 249–281.
4. Baan,R. *et al.* (2006) Carcinogenicity of carbon black, titanium dioxide, and talc. *Lancet Oncol.*, **7**, 295–296.
5. Schulte,P. *et al.* (2008) Occupational risk management of engineered nanoparticles. *J. Occup. Environ. Hyg.*, **5**, 239–249.
6. Maynard,A.D. *et al.* (2006) Safe handling of nanotechnology. *Nature*, **444**, 267–269.
7. Scheringer,M. (2008) Nanoecotoxicology: environmental risks of nanomaterials. *Nat. Nanotechnol.*, **3**, 322–323.
8. Borm,P. *et al.* (2006) Research strategies for safety evaluation of nanomaterials, part V: role of dissolution in biological fate and effects of nanoscale particles. *Toxicol. Sci.*, **90**, 23–32.
9. Phalen,R.F. (1976) Inhalation exposure of animals. *Environ. Health Perspect.*, **16**, 17–24.

934

10.Mauderly,J.L. (1997) Relevance of particle-induced rat lung tumors for assessing lung carcinogenic hazard and human lung cancer risk. *Environ. Health Perspect.*, **105** (suppl. 5), 1337–1346.

11.Roller,M. *et al.* (2006) Lung tumor risk estimates from rat studies with not specifically toxic granular dusts. *Ann. N. Y. Acad. Sci.*, **1076**, 266–280.

12.Imaida,K. *et al.* (1996) Initiation-promotion model for assessment of carcinogenicity: medium-term liver bioassay in rats for rapid detection of carcinogenic agents. *J. Toxicol. Sci.*, **21**, 483–487.

13.IARC (1999) The use of short-and medium-term tests for carcinogens and data on genetic effects in carcinogenic hazard evaluation. Consensus report. *IARC Sci. Publ.*, **146**, 1–18.

14.Asamoto,M. *et al.* (2000) Transgenic rats carrying human c-Ha-ras proto-oncogenes are highly susceptible to N-methyl-N-nitrosourea mammary carcinogenesis. *Carcinogenesis*, **21**, 243–249.

15.Han,B.S. *et al.* (2002) Inhibitory effects of 17beta-estradiol and 4-n-octylphenol on 7,12-dimethylbenz[a]anthracene-induced mammary tumor development in human c-Ha-ras proto-oncogene transgenic rats. *Carcinogenesis*, **23**, 1209–1215.

16.Ohnishi,T. *et al.* (2007) Possible application of human c-Ha-ras proto-oncogene transgenic rats in a medium-term bioassay model for carcinogens. *Toxicol. Pathol.*, **35**, 436–443.

17.Terpos,E. *et al.* (2005) Significance of macrophage inflammatory protein-1 alpha (MIP-1alpha) in multiple myeloma. *Leuk. Lymphoma*, **46**, 1699–1707.

18.Driscoll,K.E. *et al.* (1993) Macrophage inflammatory proteins 1 and 2: expression by rat alveolar macrophages, fibroblasts, and epithelial cells and in rat lung after mineral dust exposure. *Am. J. Respir. Cell Mol. Biol.*, **8**, 311–318.

19.Hamaguchi,T. *et al.* (2006) Establishment of an apoptosis-sensitive rat mammary carcinoma cell line with a mutation in the DNA-binding region of p53. *Cancer Lett.*, **232**, 279–288.

20.IARC (1989) Titanium dioxide. *IARC monograph Evaluation of carcinogenic risks to humans*. IARC Scientific Publications, Lyon, vol. 47, pp. 307–326.

21.Stoner,G.D. *et al.* (1993) Lung tumors in strain A mice: application for studies in cancer chemoprevention. *J. Cell. Biochem. Suppl.*, **17F**, 95–103.

22.Pitot,H.C. *et al.* (1978) Biochemical characterisation of stages of hepatocarcinogenesis after a single dose of diethylnitrosamine. *Nature*, **271**, 456–458.

23.Peraino,C. *et al.* (1971) Reduction and enhancement by phenobarbital of hepatocarcinogenesis induced in the rat by 2-acetylaminofluorene. *Cancer Res.*, **31**, 1506–1512.

24.Ito,N. *et al.* (2003) A medium-term rat liver bioassay for rapid *in vivo* detection of carcinogenic potential of chemicals. *Cancer Sci.*, **94**, 3–8.

25.Ito,N. *et al.* (1988) Wide-spectrum initiation models: possible applications to medium-term multiple organ bioassays for carcinogenesis modifiers. *Jpn. J. Cancer Res.*, **79**, 413–417.

26.IARC (1980) Long-term and short-term screening assays for carcinogens: a critical appraisal. *IARC Scientific Publications, Lyon, vol. 83* (suppl. 2), pp. 1–146.

27.Konishi,Y. *et al.* (1987) Lung carcinogenesis by N-nitrosobis(2-hydroxypropyl)amine-related compounds and their formation in rats. *IARC Sci. Publ.*, **82**, 250–252.

28.Nishikawa,A. *et al.* (1994) Effects of cigarette smoke on N-nitrosobis(2-oxopropyl)amine-induced pancreatic and respiratory tumorigenesis in hamsters. *Jpn. J. Cancer Res.*, **85**, 1000–1004.

29.Yamanaka,K. *et al.* (1996) Exposure to dimethylarsinic acid, a main metabolite of inorganic arsenics, strongly promotes tumorigenesis initiated by 4-nitroquinoline 1-oxide in the lungs of mice. *Carcinogenesis*, **17**, 767–770.

30.Rom,W.N. *et al.* (1991) Cellular and molecular basis of the asbestos-related diseases. *Am. Rev. Respir. Dis.*, **143**, 408–422.

31.Heppleston,A.G. (1984) Pulmonary toxicology of silica, coal and asbestos. *Environ. Health Perspect.*, **55**, 111–127.

32.Renwick,L.C. *et al.* (2001) Impairment of alveolar macrophage phagocytosis by ultrafine particles. *Toxicol. Appl. Pharmacol.*, **172**, 119–127.

33.Rimal,B. *et al.* (2005) Basic pathogenetic mechanisms in silicosis: current understanding. *Curr. Opin. Pulm. Med.*, **11**, 169–173.

34.Wang,Y. *et al.* (2007) The role of the NADPH oxidase complex, p38 MAPK, and Akt in regulating human monocyte/macrophage survival. *Am. J. Respir. Cell Mol. Biol.*, **36**, 68–77.

35.Bhatt,N.Y. *et al.* (2002) Macrophage-colony-stimulating factor-induced activation of extracellular-regulated kinase involves phosphatidylinositol 3-kinase and reactive oxygen species in human monocytes. *J. Immunol.*, **169**, 6427–6434.

36.Dorger,M. *et al.* (2000) Comparison of the phagocytic response of rat and hamster alveolar macrophages to man-made vitreous fibers *in vitro*. *Hum. Exp. Toxicol.*, **19**, 635–640.

37.Blake,T. *et al.* (1998) Effect of fiber length on glass microfiber cytotoxicity. *J. Toxicol. Environ. Health A*, **54**, 243–259.

38.Kabir,S. *et al.* (1995) Serum levels of interleukin-1, interleukin-6 and tumour necrosis factor-alpha in patients with gastric carcinoma. *Cancer Lett.*, **95**, 207–212.

39.Schneider,M.R. *et al.* (2000) Interleukin-6 stimulates clonogenic growth of primary and metastatic human colon carcinoma cells. *Cancer Lett.*, **151**, 31–38.

40.Asselin-Paturel,C. *et al.* (1998) Quantitative analysis of Th1, Th2 and TGF-beta1 cytokine expression in tumor, TIL and PBL of non-small cell lung cancer patients. *Int. J. Cancer*, **77**, 7–12.

41.Matanic,D. *et al.* (2003) Cytokines in patients with lung cancer. *Scand. J. Immunol.*, **57**, 173–178.

42.Brichory,F.M. *et al.* (2001) An immune response manifested by the common occurrence of annexins I and II autoantibodies and high circulating levels of IL-6 in lung cancer. *Proc. Natl Acad. Sci. USA*, **98**, 9824–9829.

43.Rollins,B.J. (1997) Chemokines. *Blood*, **90**, 909–928.

44.Zhou,Y. *et al.* (2005) The chemokine GRO-alpha (CXCL1) confers increased tumorigenicity to glioma cells. *Carcinogenesis*, **26**, 2058–2068.

45.Yang,G. *et al.* (2006) The chemokine growth-regulated oncogene 1 (Gro-1) links RAS signaling to the senescence of stromal fibroblasts and ovarian tumorigenesis. *Proc. Natl Acad. Sci. USA*, **103**, 16472–16477.

46.Li,A. *et al.* (2004) Constitutive expression of growth regulated oncogene (gro) in human colon carcinoma cells with different metastatic potential and its role in regulating their metastatic phenotype. *Clin. Exp. Metastasis*, **21**, 571–579.

47.Rollins,B.J. (2006) Inflammatory chemokines in cancer growth and progression. *Eur. J. Cancer*, **42**, 760–767.

48.Lentzsch,S. *et al.* (2003) Macrophage inflammatory protein 1-alpha (MIP-1 alpha) triggers migration and signaling cascades mediating survival and proliferation in multiple myeloma (MM) cells. *Blood*, **101**, 3568–3573.

49.Baggs,R.B. *et al.* (1997) Regression of pulmonary lesions produced by inhaled titanium dioxide in rats. *Vet. Pathol.*, **34**, 592–597.

50.Tsuda,H. *et al.* (2001) High susceptibility of transgenic rats carrying the human c-Ha-ras proto-oncogene to chemically-induced mammary carcinogenesis. *Mutat. Res.*, **477**, 173–182.

Biodegradation of C_{60} Fullerene Nanowhiskers by Macrophage-like Cells

SHIN-ICHI NUDEJIMA, KUN'ICHI MIYAZAWA
Fullerene Engineering Group, Exploratory Nanotechnology Research Laboratory
National Institute for Materials Science (NIMS)
1-1 Namiki, Tsukuba, Ibaraki, 305-0044
JAPAN
JUNKO OKUDA-SHIMAZAKI, AKIYOSHI TANIGUCHI
Advanced Medical Material Group, Biomaterials Center
National Institute for Materials Science (NIMS)
1-1 Namiki, Tsukuba, Ibaraki, 305-0044
JAPAN
NUDEJIMA.Shinichi@nims.go.jp   http://www.nims.go.jp/fullerene/index/index.html

Abstract: To evaluate the biological impact of C_{60} fullerene nanowhiskers (C_{60}NWs), an interaction between phorbol 12-myristate 13-acetate (PMA)-treated THP-1 cells (macrophage-like cells) and the C_{60}NWs was investigated in this study. The macrophage-like cells were exposed to 10 μg/mL of C_{60}NWs with an average length of about 6.0 μm and an average diameter of 660 nm. After 1, 3, 6, 12, 24 and 48 h of the exposure, the cells were fixed, stained with Hoechst 33342 and rhodamine-phalloidin and were observed by a differential interference contrast and confocal laser scanning microscope to estimate an uptake rate of C_{60}NWs into cells. To assess the biodegradability of C_{60}NWs by the macrophage-like cells, the cells and the exposed C_{60}NWs were observed by an inverted optical phase-contrast microscope for 28 days after the exposure. After the long-term co-culture of cells and C_{60}NWs, the cells were decomposed by proteinase K and the exposed C_{60}NWs were observed with an optical microscope and a scanning electron microscope to examine the change of C_{60}NWs by the cells. The macrophage-like cells internalized the C_{60}NWs with time and more than 70% of the cells internalized the C_{60}NWs after 48-h exposure. After the long-term co-culture, decomposed C_{60}NWs were observed in the cells and the number of short (less than 3.0 μm in length) C_{60}NWs increased after the exposure. These results suggest that macrophages may be able to decompose C_{60}NWs into C_{60} molecules as the primary immune response.

Key-Words:Fullerene nanowhisker, Needle-like crystal, Biodegradation, Macrophage, Biological assessment, In vitro

1 Introduction

Nanomaterials possess enormous potential for wide application in various fields owing to their unique properties and some of them have already been used in daily life. Fullerene nanowhiskers (FNWs), one of the most promising nanomaterials, have needle-like structures, and are composed of the fullerene molecules that are usually bonded via van der Waals forces and are synthesized by the liquid-liquid interfacial precipitation method [1]. The FNWs are expected for various applications such as low-dimensional semiconductors, field emission tips, nanoprobes for microdevices, fiber-reinforced nanocomposites, composite elements for lubrication, and so on. But the biological impact of FNWs is not clear and should be studied before their practical use.

Carbon nanotubes (CNTs), one of the most promising nanomaterials, have also the needle-like structure like FNWs. Long CNTs may be hazardous to health and environment owing to their needle-like morphology and biopersistence like asbestos [2, 3]. The nanosized needle-like structure resembling asbestos has been suspected to induce the asbestosis via inhalation. Recent studies demonstrated that multiwalled carbon nanotubes (MWCNTs) reached the subpleura in mice after the inhalation administration of MWCNTs [4]. By the exposure of mesothelioma lining of the body cavity of mice to MWCNTs, an asbestos-like pathogenic behavior associated with CNTs was observed, indicating a structure-activity relationship based on the length, to which asbestos and other pathogenic fibers show [2].

It is important to know whether the needle-like nanomaterials are decomposed in organisms or not,

89

because the biodegradable needle-like nanomaterials are considered not to harm the organisms [3, 5]. Hence, the biodegradation properties of C_{60}NWs are required for the biological assessment.

Macrophages are one of the immune system cells and defend the host against the foreign substances in a nonspecific manner during the early phase of infection. THP-1 is a human acute monocytic leukemia cell line and it is well known that the THP-1 cells are induced to differentiate into macrophage-like cells by treatment with PMA [6]. In our previous pilot study, we observed the macrophage-like cells exposed to 0.1, 1 and 10 μg/mL of the C_{60}NWs with the average length of 6.0 μm and the average diameter of 660 nm by an inverted optical phase-contrast microscope for 48 h [7]. The macrophage-like cells were observed to internalize the C_{60}NWs gradually, but the exposed C_{60}NWs didn't affect the cellular morphology. The C_{60}NWs may not exert the affect which is similar to the needle-like structure if macrophages decompose them.

In this study, we estimated the uptake rate of C_{60}NWs by macrophage-like cells in detail and assessed the biodegradability of C_{60}NWs by the cells as one of the biodegradation assessments of the C_{60}NWs in organisms.

2 Materials and Methods
2.1 Materials
2.1.1 C₆₀NWs
C_{60}NWs were synthesized by the liquid-liquid interfacial precipitation method using a C_{60}-saturated toluene solution and isopropyl alcohol [1, 7]. The length of C_{60}NWs ranged from 1 to 17 μm with an average of 6.0 μm and their diameter ranged from 300 to 1340 nm with an average of 660 nm.

2.1.2 Macrophage-like cells
THP-1 cells were purchased from American Type Culture Collection (ATCC, VA, USA). The THP-1 cells were cultured in a RPMI1640 medium (Invitrogen, CA, USA) supplemented with 10% heat inactivated fetal bovine serum (FBS, JRH Biosciences, KS, USA), 100 units/mL penicillin and 100 μg/mL streptomycin (Nacalai Tesque, Japan) (culture solution) at 37°C in an atmosphere of 5% CO_2 and saturated humidity. The THP-1 cells were subcultured every three or four days, where the number of cells in culture was maintained by centrifugation (at 1000 rpm for 3 min) and subsequent resuspension at 2×10^5 viable cells/mL. The THP-1 cells were induced to

differentiate into macrophage-like cells by treatment with 10 nM of PMA (Wako Pure Chemicals, Japan) for 24 h at 37°C in an atmosphere of 5% CO_2 and saturated humidity [7].

2.2 Methods
2.2.1 Exposure to C₆₀NWs
C_{60}NWs were dispersed in the culture solution with a concentration of 1 mg/mL [7]. The macrophage-like cells were exposed to the C_{60}NWs' suspension with the final concentration of 10 μg/mL C_{60}NWs that was adjusted by ultrasonic agitation.

2.2.2 Phagocytosis assay of C₆₀NWs
2×10^5 THP-1 cells were induced to differentiate into macrophage-like cells by PMA on a cover glass (12-545-85, Thermo Fisher Scientific, MA, USA) in 2 mL of culture solution inside a 35 mm polystyrene culture dish (Greiner Bio-One, Germany). The macrophage-like cells were exposed to 20 μL of the C_{60}NWs' suspension. After 1, 3, 6, 12, 24 and 48 h of the exposure, the macrophage-like cells were fixed by 4% paraformaldehyde (Muto Pure Chemicals, Japan) and stained with rhodamine-phalloidin (Sigma-Aldrich, MO, USA) and Hoechst 33342 (Wako Pure Chemicals, Japan). The macrophage-like cells were observed with a differential interference contrast and confocal laser scanning microscope (TCS SP5, Leica Microsystems, Germany) to locate three-dimentionally the position of C_{60}NWs.

2.2.3 Observation of C₆₀NWs in Macrophage-like cells
2×10^5 THP-1 cells were induced to differentiate into macrophage-like cells by PMA in 2 mL of culture solution in the 35 mm polystyrene culture dish. The macrophage-like cells were exposed to 20 μL of the C_{60}NWs suspension. Half of the medium was replaced by a new medium (10 nM PMA, 100 μg/mL penicillin, 100 units/mL streptomycin and 10% heat inactivated FBS in RPMI1640) every day for 28 days after the exposure for one day. The macrophage-like cells and C_{60}NWs were observed by an inverted optical phase-contrast microscope (DMIL-HC, Leica Microsystems, Germany) every day before the medium replacement. As a control experiment, the macrophage-like cells that were not exposed to C_{60}NWs and the C_{60}NWs in the PMA-containing medium were observed by the inverted optical phase-contrast microscope every day before the medium replacement.

2.2.4 Observation of the C₆₀NWs after exposure
1×10^5 THP-1 cells were induced to differentiate into macrophage-like cells in 1 mL of culture solution

using a cell culture insert (0.4 μm of pore size, Millipore, MA, USA) hanged from the top edge of a 6-well plate (Greiner bio-one, Germany) (Fig. 1). 4 mL medium was used (1 mL in the cell culture insert and the other 3 mL in the 6-well dish). The macrophage-like cells were exposed to 10 μL of the C_{60}NWs suspension. 0.5 mL of PMA-containing medium was poured into the cell culture insert after removing 0.5 mL of old medium from the 6-well plate every day for 28 days. Immediately and 28 days after the exposure, the macrophage-like cells were decomposed by 4 mL of proteinase K (Wako Pure Chemicals, Japan) with a concentration of 200 μg/mL at 50°C for 3 h after washing the cells twice with 4 mL of PBS buffer. The C_{60}NWs were washed with 4 mL of ultrapure water twice on the membrane of cell culture insert. The change of C_{60}NWs was observed with an optical microscope (ECLIPSE ME 600, Nikon, Japan) to measure the length. The morphological change of C_{60}NWs was observed with a scanning electron microscope (SEM, JSM-6700, JEOL, Japan) after coating the membrane of cell culture insert with Pt for 1 min by a deposition apparatus (ESC-101, ELIONIX, Japan). C_{60}NWs were dispersed in a PMA-containing medium as a control experiment. The change of C_{60}NWs was similarly observed as above.
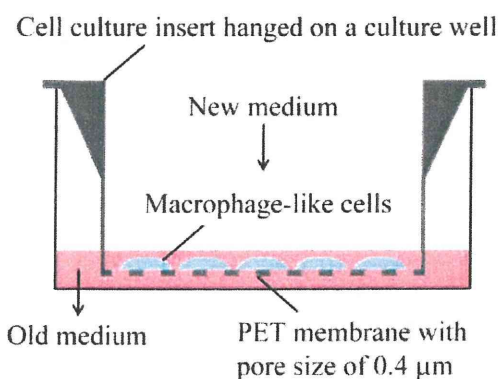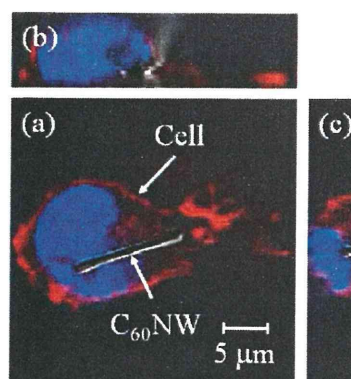

Fig.2. Confocal laser microscopy images with differential interference contrast of the macrophage-like cells exposed to the C_{60}NWs for 24 h. (a) Horizontal cross section, (b) and (c) vertical cross sections. The nucleus and F-actin are shown in blue (Hoechst 33342) and in red (rhodamine-phalloidin), respectively. The Hoechst 33342 was excited with light of 405 nm wavelength and the emission was monitored at 420-520 nm. The rhodamine-phalloidin was excited at 543 nm and the emission was monitored at 560-700 nm.
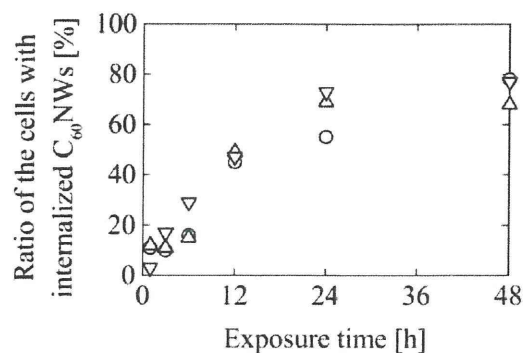

Fig.3. Ratio of the macrophage-like cells with internalized C_{60}NWs. 100 macrophage-like cells were observed for each point.

Fig.1. Macrophage-like cells were cultivated on a PET membrane with C_{60}NWs.

3 Results

3.1 Phagocytosis assay of C_{60}NWs

As shown in Fig. 2, the C_{60}NWs were phagocytized by the macrophage-like cells. The macrophage-like cells internalized the C_{60}NWs with time and more than 70% of the cells internalized them after 48 h exposure to 10 μg/mL of C_{60}NWs (Fig. 3).

3.2 Biodegradation assessment of C_{60}NWs

After the long-term co-culture of macrophage-like cells and C_{60}NWs, decomposed C_{60}NWs were observed in the cells (Fig. 4).

A change of length distribution of C_{60}NWs was estimated (Fig. 5). The number of short (less than 3.0 μm in length) C_{60}NWs increased after the co-culture with the macrophage-like cells for 28 days (Fig. 6). In contrast, at the control experiment, an increase of the

91

number of short C_{60}NWs was not observed.

The change of C_{60}NWs' morphology was not observed in the medium for 28 days (Fig. 7). On the other hand, granular crystals were observed on the membrane after the co-culture of macrophage-like cells and C_{60}NWs for 28 days.
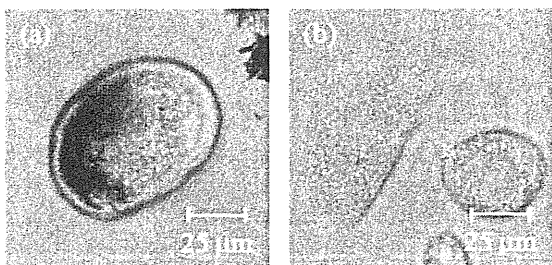

Fig.4. (a) Macrophage-like cells cultivated (a) with and (b) without C_{60}NWs for 21 days after the exposure to C_{60}NWs.

4 Discussion

4.1 Uptake of C_{60}NWs

Macrophages have a role to recognize, internalize and digest foreign materials. The uptake of foreign materials depends on their size and surface properties [8]. C_{60} is phagocytized by macrophages [9] and the uptake rate of C_{60} is lower than that of graphite particles [10].

The C_{60}NWs were also phagocytized by macrophage-like cells and the macrophage-like cells internalized the C_{60}NWs with time and more than 70% of the cells internalized them after 48 h of exposure to 10 μg/mL of C_{60}NWs. However, in our previous study, no alteration of cellular morphology was observed in the macrophage-like cells exposed to C_{60}NWs [7]. The macrophage-like cells were able to internalize the C_{60}NWs without their alteration of cellular morphology.

4.2 Biodegradation of C_{60}NWs

After the long-term co-culture of macrophage-like cells and C_{60}NWs, decomposed C_{60}NWs were observed in the cells and the number of short (less than 3.0 μm in length) C_{60}NWs increased. In addition, the change of C_{60}NWs' morphology was observed after the co-culture with the macrophage-like cells. It is unlikely that these observed substances were composed of the materials derived from the culture medium and washing buffer, because a sufficient amount of water was used for the final wash of C_{60}NWs after the treatment with the enzyme in order to decompose the macrophage-like cells and these
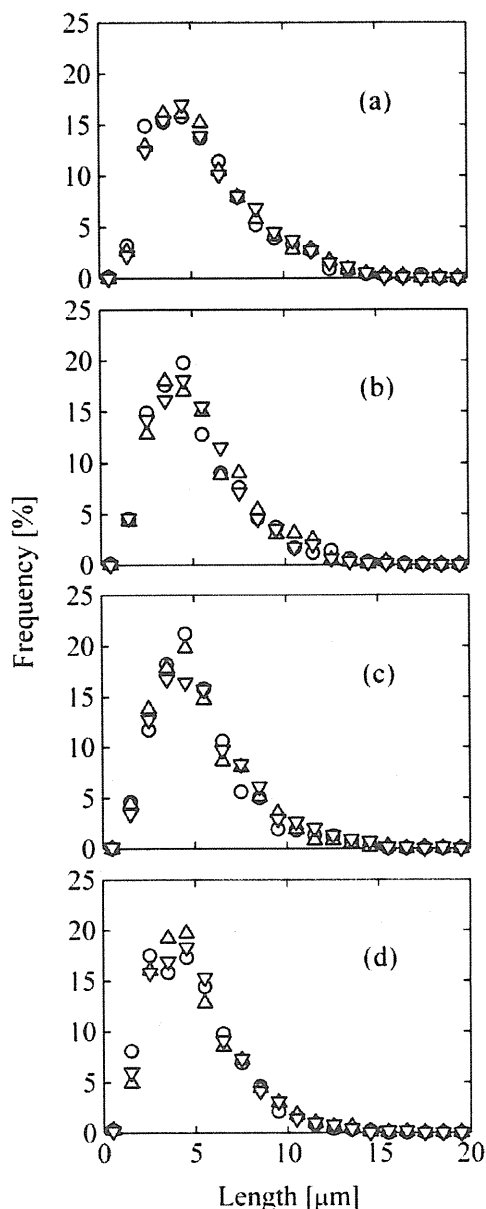

Fig.5. Length distribution of C_{60}NWs. (a) immediately after the exposure of culture medium to C_{60}NWs, (b) immediately after the exposure of macrophage-like cells to C_{60}NWs, (c) 28 days after the exposure of culture medium to C_{60}NWs and (d) 28 days after the exposure of macrophage-like cells to C_{60}NWs. The length was measured by an optical microscope after the enzymatic treatment and washing on the cell culture insert. Each symbols were expressed by measuring the length of about 1000 C_{60}NWs.
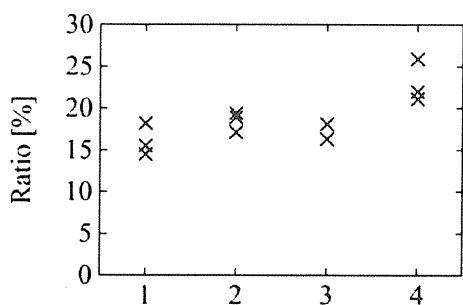
Fig.6. The ratio of short (less than 3.0 μm in length) C_{60}NWs. 1: Immediately after the exposure of culture medium to C_{60}NWs (Fig. 5 (a)). 2: Immediately after the exposure of macrophage-like cells to C_{60}NWs (Fig. 5 (b)). 3: 28 days after the exposure of culture medium to C_{60}NWs (Fig. 5 (c)). 4: 28 days after the exposure of macrophage-like cells to C_{60}NWs (Fig.5 (d)). Each point was expressed by measuring the length of about 1000 C_{60}NWs.
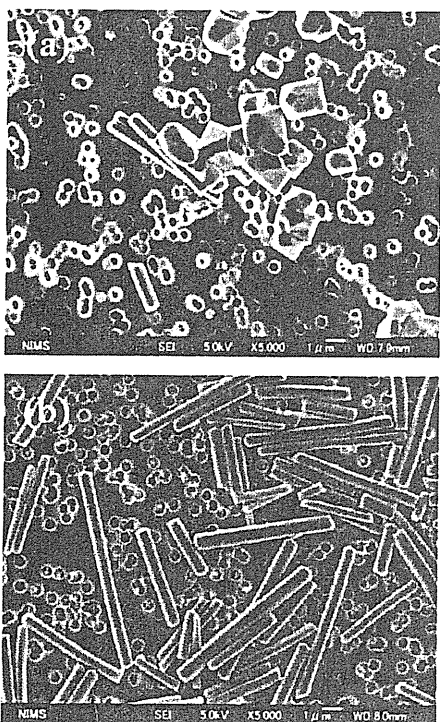

Fig.7. SEM images of the substances on the cell culture insert after the 28 days' exposure of (a) the macrophage-like cells and (b) the culture medium to C_{60}NWs.

substances were not observed at the control experiment. Hence, it is suggested that these substances are composed of fullerene molecules derived from the C_{60}NWs. It is considered that the macrophage-like cells decompose C_{60}NWs into individual C_{60} molecules and that those observed granular substances must have recrystallized from these C_{60} molecules via a dissolution-recrystallization process during the long-term co-culture or upon the enzymatic treatment.

These results suggest that the C_{60}NWs may decompose into individual C_{60} molecules by macrophages owing to the weak van der Waals bonding forces acting between the C_{60} molecules of C_{60}NWs. On the basis of this assumption, the C_{60}NWs may exert the effect which is not similar to that of the needle-like structure but is similar to that of fullerene molecules on organisms. Previous studies have reported that C_{60} (the aggregate size was not described or larger than 1 μm) were nontoxic against mammalian cells [10, 11, 12]. The C_{60}NWs may also be nontoxic against organisms. Hence, the C_{60}NWs are expected for various applications not only in the engineering fields but also in the biological field such as drug delivery systems and tissue engineering.

In this study, we demonstrated that the macrophage-like cells decompose C_{60}NWs. However, the mechanism is not clear. Recent studies show human neutrophils generate not only reactive oxygen species but also ozone in bacterial killing and inflammation [13, 14]. Additionally, there has been considerable research on the THP-1 [15]. We are going to carry out further research on the biodegradation mechanism of C_{60}NWs by the macrophage-like cells and on the biological impact (cell viability, LDH, cytokines, active oxygen and ozone generation, and so on) of C_{60}NWs using short and long C_{60}NWs.

5 Conclusion

The interaction between macrophage-like cells and C_{60}NWs was investigated in this study. Macrophage-like cells were exposed to 10 μg/mL of C_{60}NWs with an average length of about 6.0 μm and an average diameter of 660 nm. The macrophage-like cells internalized the C_{60}NWs with time and more than 70% of the cells internalized the C_{60}NWs after 48-h exposure. After the long-term co-culture, decomposed C_{60}NWs were observed in the macrophage-like cells and the number of short (less than 3.0 μm in length)

93

C_{60}NWs increased after the exposure. These results suggest that macrophages can decompose C_{60}NWs into individual C_{60} molecules as the primary immune response.

Acknowledgment

References:

[1] K. Miyazawa, Y. Kuwasaki, A. Obayashi and M. Kuwabara, C_{60} nanowhiskers formed by the liquid-liquid interfacial precipitation method, *Journal of Materials Research*, Vol.17, No.1, 2002, pp.83-88.

[2] C. A. Poland, R. Duffin, I. Kinloch, A. Maynard, W. A. H. Wallace, A. Seaton, V. Stone, S. Brown, W. Macnee and K. Donaldson, Carbon nanotubes introduced into the abdominal cavity of mice show asbestos-like pathogenicity in a pilot study, *Nature Nanotechnology*, Vol.3, 2008, pp.423-428.

[3] K. Donaldson, R. Aitken, L. Tran, V. Stone, R. Duffin, G. Forrest and A. Alexander, Carbon Nanotubes: A Review of Their Properties in Relation to Pulmonary Toxicology and Workplace Safety, *Toxicological Sciences*, Vol.92, No.1, 2006, pp.5-22.

[4] J. P. Ryman-Rasmussen, M. F. Cesta, A. R. Brody, J. K. Shipley-Phillips, J. I. Everitt, E. W. Tewksbury, O. R. Moss, B. A. Wong, D. E. Dodd, M. E. Andersen and J. C. Bonner, Inhaled carbon nanotubes reach the subpleural tissue in mice, *Nature Nanotechnology*, Vol.4, 2009, pp.747-751.

[5] R. O. McClellan and T. W. Hesterberg, Role of Biopersistence in the Pathogenicity of Man-made Fibers and Methods for Evaluating Biopersistence: A Summary of Two Round-table Discussions, *Environmental Health Perspectives*, Vol.102, No.Supplement 5, 1994, pp.277-283.

[6] S. Tsuchiya, Y. Kobayashi, Y. Goto, H. Okumura, S. Nakae, T. Konno and K. Tada, Induction of Maturation in Cultured Human Monocytic Leukemia Cells by a Phorbol Diester, *Cancer Research*, Vol.42, 1982, pp.1530-1536.

[7] S. Nudejima, K. Miyazawa, J. Okuda-Shimazaki and A. Taniguchi, Observation of phagocytosis of fullerene nanowhiskers by PMA-treated THP-1 cells, *Journal of Physics: Conference Series*, Vol.159, 2009, pp.012008.

[8] Y. Tabata and Y. Ikada, Effect of the size and surface charge of polymer microspheres on their phagocytosis by macrophage, *Biomaterials*, Vol.9, 1988, pp.356-362.

[9] A. E. Porter, K. Muller, J. Skepper, P. Midgley, M. Welland, Uptake of C_{60} by human monocyte macrophages, its localization and implications for toxicity: Studied by high resolution electron microscopy and electron tomography, *Acta Biomaterialia*, Vol.2, 2006, pp.409-419.

[10] S. Fiorito, A. Serafino, F. Andreola, P. Bernier, Effects of fullerenes and single-wall carbon nanotubes on murine and human macrophages, *Carbon*, Vol.44, 2006, pp.1100-1105.

[11] F. Moussa, P. Chretien, P. Dubois, L. Chuniaud, M. Dessante, F. Trivin, P. Y. Sizaret, V. Agafonov, R. Ceolin, H. Szwarc, V. Greugny, C. Fabre, A. Rassat, The Influence of C_{60} Powders on Cultured Human Leukocytes, *Fullerene Science & Technology*, Vol.3, No.3, 1995, pp.333-342.

[12] T. Baierl, E. Drosselmeyer, A. Seidel and S. Hippeli, Comparison of immunological effects of Fullerene C_{60} and raw soot from Fullerene production on alveolar macrophages and macrophage like cells in vitro, *Experimental and Toxicologic Pathology*, Vol.48, 1996, pp.508-511.

[13] P. Wentworth Jr., J. E. McDunn, A. D. Wentworth, C. Takeuchi, J. Nieva, T. Jones, C. Bautista, J. M. Ruedi, A. Gutierrez, K. D. Janda, B. M. Babior, A. Eschenmoser, R. A. Lerner, Evidence for Antibody-Catalyzed Ozone Formation in Bacterial Killing and Inflammation, *Science*, Vol.298, 2002, pp.2195-2199.

[14] K. Yamashita, T. Miyoshi, T. Arai, N. Endo, H. Itoh, K. Makino, K. Mizugishi, T. Uchiyama and M. Sasada, Ozone production by amino acids contributes to killing of bacteria, *Proceedings of the National Academy of Science of the United States of America*, Vol.105, No.44, 2008, pp.16912-16917.

[15] The FANTOM Consortium and the Riken Omics Science Center, The transcriptional network that controls growth arrest and differentiation in a human myeloid leukemia cell line, *Nature Genetics*, Vol.41, No.5, 2009, pp.553-562.

SYMPOSIUM PRESENTATION

Risk Assessment Studies of Nanomaterials in Japan and Other Countries

Hiroyuki Tsuda

Abstract

Recent developments in nanoparticle (NP) technology and their commercial production have raised concern regarding NP risk to health and the environment. The toxicological characteristics of NP may not be similar to that observed in pre-NP materials because of the enormous differences in size and surface area. Thus, careful risk evaluation studies are required. Since some NP have already been produced and introduced into the market, before a suitable framework enabling risk management has been firmly established, toxicological studies based on the specificity of NP which are not subordinate to their commercial production are indispensable. The summary of nanotoxicology studies shown below clearly indicates that compared with the UK, EU, USA, and other countries, Japanese studies regarding metals and SWCNT are far from sufficient to evaluate risk.

Key Words: Nanoparticles - toxicology - carcinogenicity - titanium dioxide - carbon black

Introduction

The safety of our living environment can be secured by the balanced function of three elements: risk assessment, risk management and risk communication. The first of these elements, risk assessment, must be addressed first, since without reliable risk assessment, risk communication and risk management can not function. Importantly, for reliable risk assessment long-term animal studies are indispensable.

These principles, of course, hold true for engineered nanoparticles. Unfortunately, the risk assessment data for engineered nanoparticles are rather fragmentary. However, the available findings do present a disturbing picture of potential carcinogens entering the market place. Engineered nanoparticles included in this review include nano-size titanium dioxide ($nTiO_2$), carbon black (nCB), single-walled carbon nanotubes (SWCNT), multiple-walled carbon nanotubes (MWCNT) and fullerenes

Table 1. Number of Subacute/Chronic Toxicity Tests (PubMed, ~2007)

	●	■	☰	Total
TiO_2	1	2	2[a]	4 5
S/MW-CNT	2			6 2
Fullerenes		1		1
Uf-Carbon black			4[a]	4
Total	0	3	6	9

[a]Carcinogenic

(C60). A summary of the testing so far performed shows that data are limited and Japan is not putting the priority this subject deserves (see Table 1) and Tsuda et al (2009), for a review.

Overall Evaluation and Proposal for the Future

During the development and marketing of nanomaterials, risk assessment of these new products has been perfunctory at best. While nanomaterials have undeniable benefits, their use also has undeniable potential risk. This risk must be addressed in an unbiased and thorough manner. Only after the toxicity of the various nanomaterials is understood can their true benefits be realized.

In rodent studies, $nTiO_2$ whether administered by inhalation or intratracheal instillation was shown to induce lung tumors with characteristic squamous cell morphology in female rats. These nanomaterials did not induce lung tumors in male rats. Our own studies have also shown that instillation of $nTiO_2$ into the lungs of female rats showed tumor promoting activity and resulted in elevated ROS-mediated damage and production of inflammatory cytokines. It is reasonable to assume that other metal-derived nanoparticles, such as aluminium and copper nanoparticles, and metal containing nanoparticles, for example nCB-metal mixtures and SWCNT and MWCNT preparations, are also capable of producing these effects.
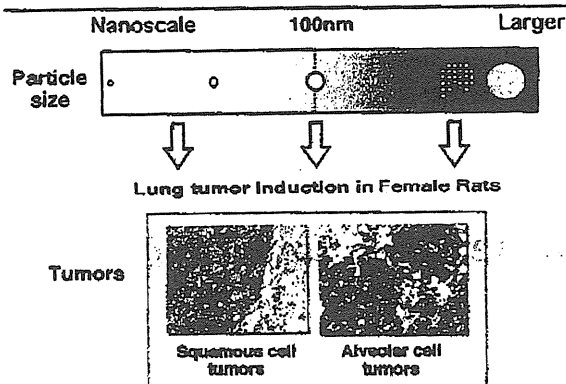
Nanotoxicology Project, Department of Molecular Toxicology, Nagoya City University Graduate School of Medical Sciences 1 Kawasumi, Mizuho-cho, Mizuho-ku, Nagoya 467-8601, Japan

Figure 1. Schematic Presentation of Carcinogenic Effects of TiO_2, Carbon Black. Carcinogenic effects were elicited by both nano-scale and larger sized particles

Nanoparticles such as $nTiO_2$, nCB, SWCNT and MWCNT when intratracheally administered, were detected by light microscope as aggregates or agglomerates and these forms are reported to induce foreign body granulation tissue with various degree of inflammatory reaction. Although the relevance of foreign body-induced chronic inflammation to carcinogenesis is not clearly established, it is possible that reactive oxygen species (ROS) produced by macrophages attempting to destroy the foreign material in the inflammation site may cause DNA damage associated with carcinogenesis. Another possible contributing factor is metal, for example from metal-derived nanoparticles such as TiO_2 or from metal contaminants: these metals could also be involved in ROS production. Thus, it is possible that the observed carcinogenic effect is not specific to nanoparticles but rather associated with their ability to induce persistent foreign body-induced chronic inflammation and/or introduce metals into susceptible sites. For example, TiO_2 and carbon blacks larger than 100nm in diameter are known to induce lung tumors including similar squamous cell morphology (Nikula, 2000); (Pott and Roller, 2005) and both of these materials (larger than nano size) are classified as into group 2B (possibly carcinogenic to humans) by WHO/IARC (see Figure 1).

Mechanisms for mesothelioma induction by MWCNT in mice and rats have not been elucidated yet. A possible contributing factor is metal: Transition metals, such as iron, are commonly used as a catalytic center in the formation of CNTs, and contaminating metal in SWCNT and MWCNT particles could catalyze the formation of ROS by the Fenton reaction (Liu and Okada, 1994). One example of this type of toxicity is that human keratinocytes exposed to SWCNT were killed by ROS in the media (Shvedova et al., 2003). Another possible contributing factor is the length of the MWCNT (Pott and Roller, 2005; Muller et al., 2009; Sakamoto et al., 2009).

As noted at the beginning of this review, for reliable risk assessment long-term animal studies are indispensable. This is particularly true for risk assessment of potential carcinogens. The standard for the evaluation of the carcinogenic potential of a test chemical is testing

in two rodent species, generally rats and mice, of each sex, at 3 doses (0, low and high) of the test chemical for up to two years. In the studies conducted to date concerning the carcinogenic risk presented by nanoparticles, there is a noticeable lack of long term testing: No long-term tests of any type have been reported for either SWCNT or fullerenes. Importantly, the primary goal of risk assessment is not to simply ban a product from the market place, but rather to determine product safety and establish guidelines lines for its production and use and promote consumer confidence. Given the known ability of many nanomaterials to induce mechanisms which are active in humans that are risk factors for carcinogenesis, for example ROS and inflammatory cytokine production, the continued introduction of these materials into the market is alarming. Establishing the safety of these materials is urgently needed.

In this short review, available in vivo data concerning the carcinogenic effects of $nTiO_2$, nCB, SWCNT and MWCNT, and Fullerenes is outlined. Of these, $nTiO_2$ and nCB are classified as possibly carcinogenic to humans. Testing of the carcinogenic activity of MWCNT produced mixed results. SWCNT and fullerenes have no carcinogenic activity in the studies conducted to date, however, toxicity testing of these materials has been quite limited and both of these materials have the potential to produce ROS. The observations noted here may apply to possible carcinogenic risk of other nanoparticles because of shared mechanisms of induction of inflammatory lesions and ROS generation. Our conclusions are that nanoparticles are clearly potentially toxic/carcinogenic to humans and their toxicity must be assessed, and their production and use managed appropriately.

References

Liu M, Okada S (1994). Induction of free radicals and tumors in the kidneys of Wistar rats by ferric ethylenediamine-N,N'-diacetate. *Carcinogenesis*, 15, 2817-21.

Muller J, Delos M, Panin N, et al (2009). Absence of carcinogenic response to multiwall carbon nanotubes in a 2-year bioassay in the peritoneal cavity of the rat. *Toxicol Sci*, 110, 442-8.

Muller J, Huaux F, Moreau N, et al (2005). Respiratory toxicity of multi-wall carbon nanotubes. *Toxicol Appl Pharmacol*, 207, 221-31.

Nikula KJ (2000). Rat lung tumors induced by exposure to selected poorly soluble nonfibrous particles. *Inhal Toxicol*, 12, 97-119.

Pott F, Roller M (2005). Carcinogenicity study with nineteen granular dusts in rats. *Eur J Oncol*, 10, 249.

Sakamoto Y, Nakae D, Fukumori N, et al (2009). Induction of mesothelioma by a single intrascrotal administration of multi-wall carbon nanotube in intact male Fischer 344 rats. *J Toxicol Sci*, 34, 65-76.

Shvedova AA, Castranova V, Kisin ER, et al (2003). Exposure to carbon nanotube material: assessment of nanotube cytotoxicity using human keratinocyte cells. *J Toxicol Environ Health A*, 66, 1909-26.

Tsuda H, Xu J, Sakai Y, Futakuchi M, Fukamachi K (2009). Toxicology of engineered nanomaterials - A review of carcinogenic potential. *Asian Pacific J Cancer Prev*, 10, 975-80.

—137—

ナノテクノロジーと環境リスク

西村　哲治

ナノテクノロジーと環境リスク

西村 哲治

はじめに

　20世紀後半のマイクロテクノロジーの世界から，21世紀はナノ(1nm：1mの10億分の1)テクノロジーの世界になると言われ，ナノメートルサイズのスケールで現象を理解し，物質の構造や配列を制御し，ナノメートルサイズの物質を取り扱うことにより，新しい性質や機能を利用した技術革新が期待されている．ナノサイズの物質(ナノ物質)はナノテクノロジーの重要な役割を担う新規物質・材料と考えられる．このナノサイズの物質を材料(ナノ材料)として取り扱おうとしている分野は多岐にわたっており，すでにわれわれの身の回りの一般家庭用品や食品にも使用されてきている．今後その適用範囲は拡大していくものと思われる．これらの製品を使用することで，われわれがナノ材料に直接接する機会が増加すると共に，使用後の廃棄物から環境中への放出が予想され，環境リスク評価への関心が高まっている．

　本稿では，工業用に生産，使用されるナノ材料に焦点を当てて，環境リスクについて概説する．なお，ジーゼル排ガス中に含まれるナノサイズの微粒子など，非意図的に生成されるナノ粒子に関しても重要な課題はあるが，ここでは割愛させていただく．

ナノ材料の特性

1. ナノ材料の大きさ

　工業用ナノ材料の大きさの定義は，OECDはじめ各分野で議論されているが，「長径が100nm以下の粒径を有するもの」となっている．大きさが議論の的になっているのは，これまで取り扱ってきた同重量の材料に比べ表面積が大きくなることによる物理化学的影響が異なってくる可能性が考慮されているからである．例えば，他の物質との相互作用，反応性，化学物質の吸着性が高まるのではないかと考えられている．また，機械的，光学的，磁気的，電気的，生物学的な特性も異なっていることが考えられる．これらの観点から，これまでの有害影響は化学的性状を中心として評価されてきたが，その他，物理的な側面等からも考慮しなくてはいけないと考えられている．

　一方，人への健康影響を含む生態系への影響を考慮する際に，工業用ナノ材料の単分子がナノサイズであっても，製品中または環境中でナノサイズの粒子として存在し，どの大きさの粒子として挙動するかが大きな問題となる．一例として，化粧品に使用されている酸化チタンに関して，皮膚塗布による曝露評価をする際に分散溶液中の粒径分布を測定した結果を示す．アルミナ，シリカおよびシリコーンで表面修飾した初期粒径35nmの酸化チタン(ルチル型：酸化チタン含量80%以上)を，良い分散を示すシリコーンに超音波処理

にしむら　てつじ：国立医薬品食品衛生化学部　連絡先：☎ 158-8501 東京都世田谷区上用賀 1-18-1